POLYTECHNIC INSTITUTE OF LEIRIA
SCHOOL OF TECHNOLOGY AND MANAGEMENT
MECHANICAL ENGINEERING DEPARTMENT

Methodologies for pre-processing polymeric filament for Direct Digital Fabrication

Master degree in Digital Direct Fabrication

César Miguel Coitos da Silva

Leiria, September 2022

Methodologies for pre-processing polymeric filament for Direct Digital Fabrication

Master degree in Digital Direct Fabrication

César Miguel Coitos da Silva

Project under the supervision of Professor Mário António Simões Correia and Professor Paulo Jorge Simões Coelho.

Leiria, September 2022

Originality and Copyright

This project is original, made only for this purpose, and all authors whose studies and publications were used to complete it are duly acknowledged.

Partial reproduction of this document is authorized, provided that the Author is explicitly mentioned, as well as the study cycle, i.e., Master degree in Digital Direct Fabrication, 2021/2022 academic year, of the School of Technology and Management of the Polytechnic Institute of Leiria, and the date of the public presentation of this work.

Dedication

This project work is dedicated to my wife, Susana, who has been a constant source of support and encouragement during the challenges of graduate school and life.

Acknowledgments

I would like to thank my project supervisors Professor Doutor Mário António Simões Correia and Professor Doutor Paulo Jorge Simões Coelho who were a good support in the research of contents and in the elaboration of the work, in the support in solving problems and doubts that arose. I am also grateful for the challenges that were created throughout the work, which were encouraging and empowering.

I also thank my family and friends who have supported me throughout the process, and all those who encouraged and motivated me during this journey.

Abstract

The digital age presents alternatives to more traditional manufacturing concepts. One of the alternatives most adopted by the industry and society, in general, focuses on additive manufacturing, which has improved significantly over time, improving the user interface and optimizing parts construction times and quality.

In this work is intended to study the impact of dehumidification pre-processing of the material at the Polylactic Acid (PLA) and Polyethylene Terephtalate Glycol (PETG), used in Fused Deposition Modeling (FDM). The results obtained in on the parts produced allowed to draw conclusions about impacts at an aesthetic level and at a mechanical level, and assess whether the pre-processing energy costs are justified, regarding the final quality of the produced part or improvements in their mechanical properties. Measurements of the weight were carried out on the printed pieces for the aesthetic experiments to compare the printed piece with dehumidified, non-dehumidified material, the Computer-Aided Design (CAD) part simulation and slicer software part simulation. The most significant results occurred in the aesthetic tests, as the differences are evident between the part printed with dehumidified material and the part printed with non-dehumidified material. The final weight of the pieces differs in all scenarios, where the lightest pieces are in the CAD software simulation, and heaviest parts are in the simulation of the slicer software. In the tensile tests, the non-dehumidified PLA material obtained better performance when compared to the PLA that was previously dehumidified for 6 hours. In the case of PETG, it was possible to identify the similar tensile strength between the previously dehumidified filament and the filament not previously dehumidified. To conclude the energy study revealed an overall consumption of approximately 0.32 kWh for the dehumidifier and printer set.

Keywords: FDM, PLA, PETG, Moisture, Polymers, 3D Printing.

Resumo

A era digital apresenta alternativas aos conceitos de fabrico mais tradicionais. Uma das alternativas mais adotadas pela indústria e pela sociedade, em geral, centra-se no fabrico aditivo, que tem melhorado significativamente ao longo do tempo, melhorando a interface do utilizador e otimizando os tempos e a qualidade de construção das peças.

Neste trabalho pretende-se estudar o impacto do pré-processamento de desumidificação do material Ácido Poliláctico (PLA) e do Polietileno Tereftalato de Glicol (PETG), utilizado na Modelação de Deposição de Fundido (FDM). Os resultados obtidos nas peças produzidas permitiram tirar conclusões sobre os impactos a nível estético e a nível mecânico, e avaliar se os custos energéticos do pré-processamento justificam, relativamente à qualidade final da peça produzida ou a melhorias nas suas qualidades mecânicas. Foram realizadas medições do peso nas peças impressas para as experiências estéticas, para comparar a peça impressa com material desumidificado e não desumidificado, a simulação de peças com desenho assistido por computador (CAD) e a simulação de peças com software de modelação. Os resultados mais significativos ocorreram nos testes estéticos, uma vez que as diferenças são evidentes entre a peça impressa com material desumidificado e a peça impressa com material não desumidificado. O peso final das peças difere em todos os cenários, onde as peças mais leves estão na simulação do software CAD, e as peças mais pesadas estão na simulação do software de modelação. Nos testes de tração, o material PLA não desumidificado obteve um melhor desempenho quando comparado com o PLA que foi desumidificado anteriormente durante 6 horas. No caso do PETG, foi possível identificar a resistência à tração semelhante entre o filamento previamente desumidificado e o filamento não desumidificado anteriormente. Para concluir, o estudo energético revelou um consumo global de aproximadamente 0.32 kWh para o conjunto desumidificador e impressora.

Palavras-chave: FDM, PLA, PETG, Humidade, Polímeros, Impressão 3D.

Contents

List of Figures

List of Tables

List of Abbreviations and Acronyms

ABS	Acrylonitrile Butadiene Styrene
AM	Additive Manufacturing
ASA	Acrylonitrile Styrene Acrylate
BVOH	Butenediol Vinyl Alcohol Co-polymer
CAD	Computer-Aided Design
CAM	Computer Aided Manufacturing
CHDM	Cyclohexanedimethanol
CPE	Chlorinated Polyethylene
CPS	Cyber Systems
EG	Ethylene glycol
ESTG	School of Technology and Management
FDM	Fused deposition modeling
GTAI	Germany Trade and Invest
HIPS	High Impact Polystyrene
ICSP	In-Circuit Serial Programming
ICT	Information and communication technologies
IoT	Internet of things
ME	Material Extrusion
PA6	Polyamide 6
PC	Polycarbonate
PET	Polyethylene terephthalate
PETG	Polyethylene Terephthalate Glycol
PLA	Poly-lactic Acid
PMMA	Poly(methyl methacrylate)
PP	Polypropylene
PVA	Polyvinyl Alcohol
PVB	Polyvinyl Butyral
TPA	Terephthalic acid
TPE	Thermoplastic elastomer
TPU	Thermoplastic polyurethane

UV	Ultraviolet

1. Introduction

One of the processes of additive manufacturing with great technological growth since their emergence, both in the creation of more and better raw materials and in the updating and development of equipment, is the material extrusion process. This additive manufacturing process includes the fused deposition modeling (FDM), commonly known as 3D printing, which is in enormous growth both at the corporate level, for the manufacture of prototypes, gigs and features, and parts with complex geometries, as well as in society, given the ease of learning the technique, reduced costs of equipment and materials and also the variety of geometries that can be reproduced. The fact that FDM is an additive manufacturing process, allows a material reduction compared to subtractive manufacturing, a reduction in the weight of the parts produced using the various types of fillers presented by the slicing software, and a wide variety of materials that fill a wide range of solutions at all levels [1].

The degradation of the filamentous material due to moisture is an obstacle for all producers, as it makes the filament brittle, generates problems during the production of the parts and the final part can have aesthetic defects, depending on the ease with which each raw material has to absorb moisture [2].

With this work, will be presented a study of the impact of moisture on the final pieces, both aesthetically and mechanically, with pieces made using PLA and PETG filaments, two types of filaments widely used by adepts of this technique. Also, this study aims to facilitate the process and manufacture of pieces using FDM, for all the users of the technique who have faced the obstacles created by the presence of moisture in the filaments. During the work, geometries that enhance material drag will be tested, at an aesthetic level and a mechanical level, in order to obtain relationships for the behavior of the material processed in the two scenarios.

The aesthetic method does not have any associated standard, having only the critical sense of the user, but basically, it translates into the non-appearance of incompleteness in the pieces and in the non-appearance of dragged in the final pieces. In the mechanical method, specimens were manufactured and tested according to the D638 standard [3]. For the energy cost, a device will be used that records the equipment's real-time energy consumption used for the dehumidification of the material, as well as the energy cost of using the 3D printer [4].

In this work, the theme, techniques, and processes to be studied will be introduced, all related to additive manufacturing, specifically FDM. After the introduction in chapter 1, the literature review is presented in chapter 2 which contextualizes the technique and its concept, the types of equipment used, the defects that can occur during the fabrication phase of the pieces and what the filament dehumidification consists of. Chapter 3 discusses the materials and methods used, the different types of filaments applied in the various experiments, in this case, PLA and PETG, and their properties. In the Methods subsection are represented the devices and the techniques used for the aesthetic and mechanical study of the produced pieces. This is followed by the experimental description in chapter 4, where all the experiments performed with both non-dehumidified and dehumidified material are considered. Finally, in chapter 5, we find a discussion of the results where there is an opinion of the author about the results obtained throughout the work, as well as its conclusion in chapter 6.

2. Literature review

Industry 4.0 was initially introduced during the Hannover fair in 2011 and was officially announced in 2013 as a strategic German initiative, to take a pioneering role in industries that are revolutionizing the production sector [5].

Industry 4.0 symbolizes the beginning of the fourth industrial revolution and represents the current trend in automation technologies in the manufacturing industry, including technologies such as cyber systems (CPS), the internet of things (IoT), and cloud computing. Industry 4.0 represents the technological evolution of embedded systems for cyber-physical systems. In industry 4.0, embedded systems, machine-to-machine semantic communication, IoT, and CPS technologies are integrating virtual space into the physical world, and in addition, a new generation of industrial systems is emerging, such as smart factories, to deal with the complexity of production in the cyber-physical environment. In this new technological evolution driven by information and communication technologies (ICT), embedded systems, IoT, CPS, industrial integration and industrial information integration are playing important roles [5].

2.1. **Additive manufacturing**

The technologies referred to in the previous topic help to ensure the effective use of existing information for smart manufacturing, but the physical part of smart factories is still somewhat limited by the capacity of existing manufacturing systems. This makes additive manufacturing processes one of the vital components of Industry 4.0. Given the need for mass customization in Industry 4.0 unconventional manufacturing methods are required. Thus, additive manufacturing can become an essential technology for custom product manufacturing due to its ability to create sophisticated objects with advanced attributes. Thanks to increased product quality, additive manufacturing is currently found in various sectors such as aerospace, biomedical, and manufacturing. The fact that it is a technology designed to create complex, precise, and reinforced objects with greater production speed, may offer a way to replace conventional production techniques in a near future [1].

Although the number of innovative additive manufacturing processes is increasing considerably, they come from well-established core technologies. More improved processes are likely to be developed with technological advances in additive manufacturing. However, most of these processes are designed to print common materials, such as polymers, which are generally used for non-industrial applications. Due to the need for engineering applications in the context of Industry 4.0, specific additive manufacturing processes have recently been confronted. As metals are the most commonly preferred material in the industry, the issue of additive manufacturing using metal has received considerable attention in this new era. Furthermore, the future of manufacturing is expected to guide our industry towards using these processes together. Known as hybrid manufacturing, this new phase offers a way to practice subtractive methods that accompany additives, to produce better products with higher surface quality, and fatigue resistance, among other properties. Currently, the growing interest in hybrid manufacturing leads to various combinations of manufacturing processes in addition to conventional additive manufacturing processes [1].

Since the late 80's, equipment for direct digital manufacturing has been developed, following the principle of building parts by layers, where each layer is a thin section of the part derived from the original Computer-Aided Design (CAD) data. The thinner each layer is, the closer the final part will be to the original. All commercially available additive manufacturing (AM) machines use layer-by-layer construction, where the differences lie in the type of materials they process, how the layers are created and how the layers adhere to each other. These differences have an impact on the final accuracy of the part, material properties, and mechanical properties. The difference is also present in the production speed of each component, the type of post-processing required, the size of the AM equipment used, and the overall cost of the machine and the process [6]. In Figure 1 it is possible to observe how is obtained a piece by AM.

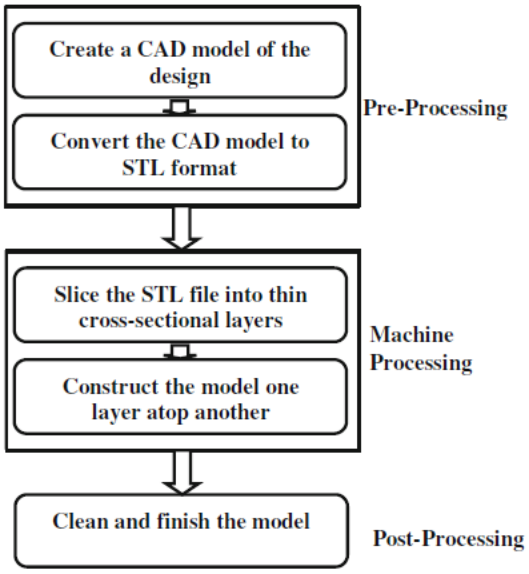

Figure 1 - Steps to obtain parts by AM techniques [7].

According to the group "ASTM F42 – Additive Manufacturing", Committee on Additive Manufacturing Technologies, the range of additive manufacturing processes has been classified into seven categories, each with a distinct procedure for obtaining the layer. Table 1 depicts the seven additive manufacturing categories, the material used, and some of their advantages and disadvantages [8].

Table 1 - Categories of Additive Manufacturing [8].

Categories of AM	Materials	Advantages	Disadvantages
VAT Photopolymerization	Plastics and polymers in resin form.	High level of accuracy; Relatively quick process.	Relatively expensive; Limited material of photo-resins.
Material Jetting	Plastics and polymers.	Low waste; Multiple material parts and colors under one process.	Support material is often required.
Binder Jetting	Metals, polymers, ceramics.	Uses a range of materials; The process is generally faster than others.	Not always suitable for structural parts.
Material Extrusion	Plastics and polymers in filament form.	Inexpensive process; Easily understandable technique.	Accuracy and speed are low when compared to other processes.
Powder Bed Fusion	Metal and polymers powder.	Relatively inexpensive; No support needed.	Lack of structural properties in materials.
Sheet Lamination	Paper, plastics, and metal in sheet form.	Low cost; Ease of material handling.	Limited material use.
Directed Energy Deposition	Metals powder.	Can be used for repairing; Reduced material waste.	Low build resolution.

The categories indicated above are part of additive manufacturing, but in this dissertation, FDM will be studied, which belongs to the material extrusion (ME) category.

2.2. **FDM**

Fused Deposition Modeling (FDM) is one of the widely accepted 3D printing techniques due to its simplified operations. The type of materials used in this technique is filament-shaped thermoplastics. As exemplified in Figure 2, the filament is electrically heated to a molten state and is extruded through a nozzle that moves along the X, and Y directions. The nozzle is mounted on the extrusion head, which is controlled by computer software, and deposits material in thin layers on the construction platform. The platform is kept at a low temperature so that it can solidify the molten thermoplastic material that exits through the nozzle [7].

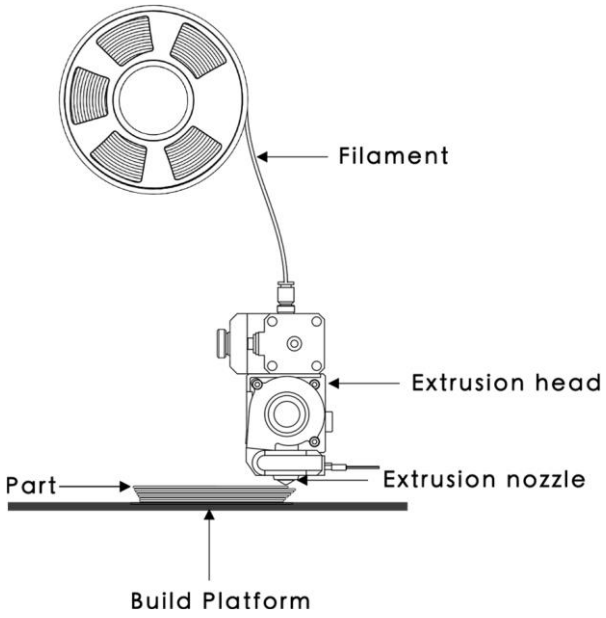

Figure 2 - The fusion deposition modeling (FDM) process [9].

In FDM the pre-processing part includes drawing using CAD software, as well as converting the model into a file for STL format, which must be exported to the printing machine for the machine to manufacture the part. After the file is sent to the machine, the part starts to be generated with the deposition of the material layer by layer. At the end of the manufacturing process, the finished part is removed from the machine and undergoes post-processing to improve its mechanical and aesthetic properties [7].

At the beginning of the manufacturing process, the extrusion head lowers the distance set for the first layer, usually 0.2 mm. Once this value is reached, the extrusion of material for the construction of the CAD model starts. The supports that help in the construction of negative zones of the part are built together with the part. After the model is printed, the supports are removed to obtain the finished part. The main advantage of the FDM process is its simplicity, reliability, and economy [7].

2.2.1. **Equipment**

- **Printers**

The machines used in FDM, 3D printers, are among the engineering products with the greatest development and expansion nowadays, due to the cost of both equipment and materials being significantly low [10]. The 3D printer is composed of mechanisms that ensure the positioning of the material extrusion nozzle at any point that is contained within the print volume possible by the printer. It is called 3D printer given the fact that it uses 3 axes for the construction of objects. The printer moves on the X axis, left and right, on the Y axis, forward and backward, and on the Z axis, up and down. In Figure 3 can be seen a cube illustrating the axis of movement of the printer [11].

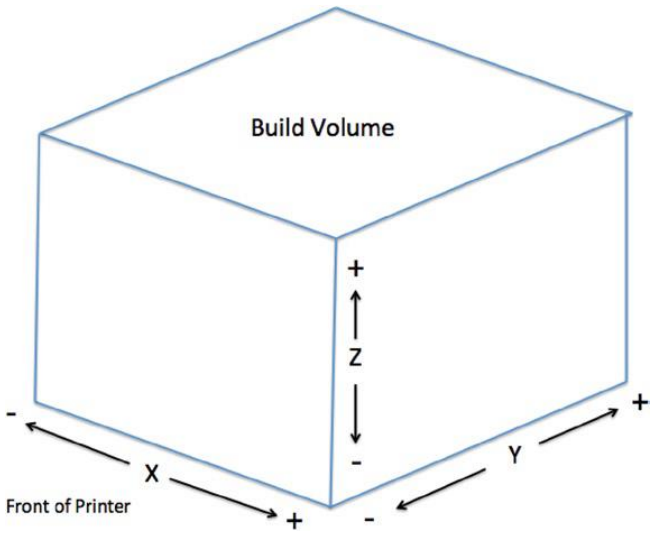

Figure 3 - Axes movement and orientation [11].

The printer mechanisms may vary, although the final result is very similar. The most important type of mechanisms used in this type of printer is described below [12].

Gantry

Printers with the Gantry mechanism, are based on the movement of the print head on the X and Y axis, while the print base moves on the Z axis. Within this system, there may be differences related to the filament extrusion mechanism. In one case the extrusion head may be coupled to the heated nozzle, making the structure to be moved heavier (it is named as direct drive) and in the other case, the extruder motor is supported on the printer structure and distanced from the nozzle, which increases the printing speed (it is named as bowden) [12]. As an example, Figure 4 presents a gantry-type printer, as described previously.

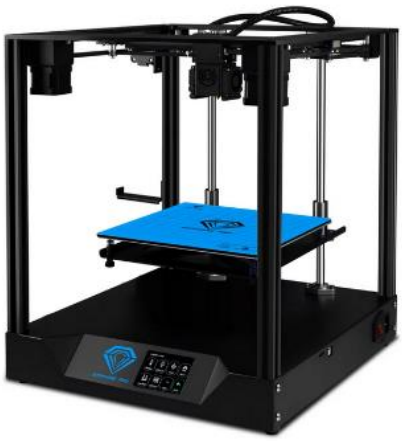

Figure 4 - Gantry printer [13].

Moving Bed

In this kind of printer, the movement in the X and Z axis is assumed by the heated nozzle. The printing surface in this concept moves on the Y axis independently. These type of printers are generally priced in the low-cost range. In addition to being slower compared to other equipment, they are easy to maintain because their system is simple to operate. This configuration of the printer can also use the direct drive or bowden extrusion mechanism [12]. Figure 5 shows a moving bed printer example.

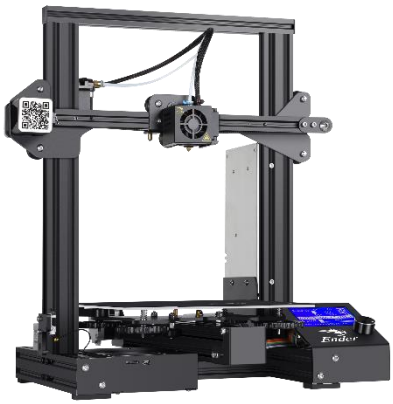

Figure 5 - Moving bed printer [14].

Deltabot

The deltabot uses 3 rods connected to the printing head, and these rods are used to move the printing head on the 3 axes, X, Y, and Z. The operating mechanism of this type of printer is similar to the pick-and-place robots used in the industry. The fact that the bowden configuration is used, allows the printer more precise and faster positioning of the heated nozzle, with relatively simple mechanics [12], as shown in Figure 6.

Figure 6 - Deltabot printer [15].

Despite the FDM process being a simple process to work with, achieving an optimal final quality of the pieces is not always an easy task.

- **Filament Dryers**

Filament dryers are complementary equipment for the FDM process, used to remove moisture from polymeric filaments. In this sector, there are different types of equipment and mechanisms for the same purpose.

Passively drying filament container

The operating principle of these devices is based on a rigid and resistant plastic box containing silica bags that absorb humidity from the material inside the box [16], as presented in Figure 7.

Figure 7 - Dry storage box [16].

The equipment in the previous figure includes a high-precision thermo-hygrometer, which indicates temperature and humidity levels inside the box [16].

Hot chamber filament dryers

This type of dryer contains a chamber where the filament reel is placed. Inside this chamber the air is heated through a heating element, previously adjusted for the material to be dried, circulating through the chamber due to a fan. The hot air flows around the polymeric filament and heats it. The excess moisture evaporates from the filament and is transported by

the air. In the dryer's hot chamber section there are air dryers that use silica to store the water particles circulating in the air (as depicted in Figure 8) and dryers without silica inside (as depicted in Figure 9). These devices can feed the printer during operation [17].

Figure 8 - Silica filament dryer [18].

Figure 9 - Silica-free filament dryer [19].

In-line systems

With in-line systems, the filament is dried in real time and only the material used is dried. This type of equipment is different from the conventional method, which dries the whole reel of material simultaneously in a chamber. In the case of this specific equipment (Figure 10 presents an example), the manufacturer recommends a pre-drying cycle of at least 50 minutes for the first portion of the material and then the filament can be used with ease and consistency [20] [21].

Figure 10 - In-line filament dryer [20].

2.2.2. **Troubleshooting and solutions for parts construction**

This topic will address some of the most important problems identified in the FDM process and suggest some solutions.

Slicer

Slicer, or CAM software, is the type of software that converts the part obtained through CAD software (STL) to a G-code file. The G-code is a file that contains the printer characteristics, the characteristics of the part to be printed and the parameters defined for the layer construction process. The G-code file must contain the correct data for the printer that will be used to print the part and must not be used on a printer with different characteristics [11].

Software errors can generate problems such as:

- stop extruding during mid print, due CAD file error or G-code error;

- extrusion away from previous layers, (known as “spaghetti monster" – as presented in Figure 11), could be an error generated by a CAD file or G-code [9].

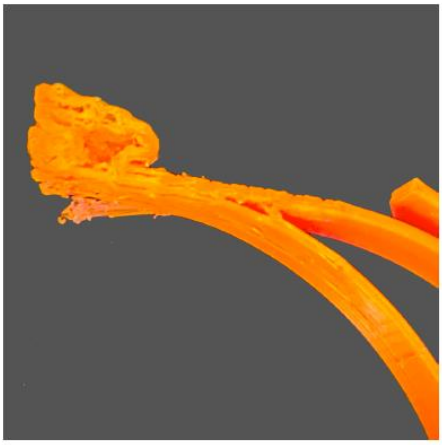

Figure 11 - Spaghetti Monster [9].

First layer

The quality of the first print layer is crucial to achieving a good construction of the printed part, and the adhesion of the first layer to the print surface is a key point [11].

The fact that the first layer does not adhere well to the print plate may be due to the following reasons: (i) the heating plate not being leveled correctly, (ii) the heating nozzle being too far from the heating plate (Figure 12) (iii) the printing speed of the first layer being too fast (iv) the heating plate adherence being too poor [9].

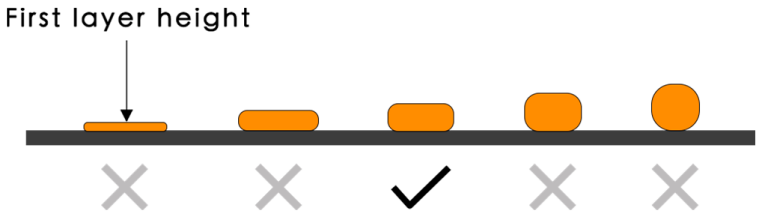

Figure 12 - Optimal first layer [9].

Some points to take into consideration to avoid poor quality of the first layer are:

- Setting up the temperature indicated by the manufacturer of the material to be used on the printing surface and starting to print the part after the defined value stabilizes;

- The use of brim when the contact surface between the piece and the heated platform has a reduced area, thus increasing its contact area, as illustrated in Figure 13;

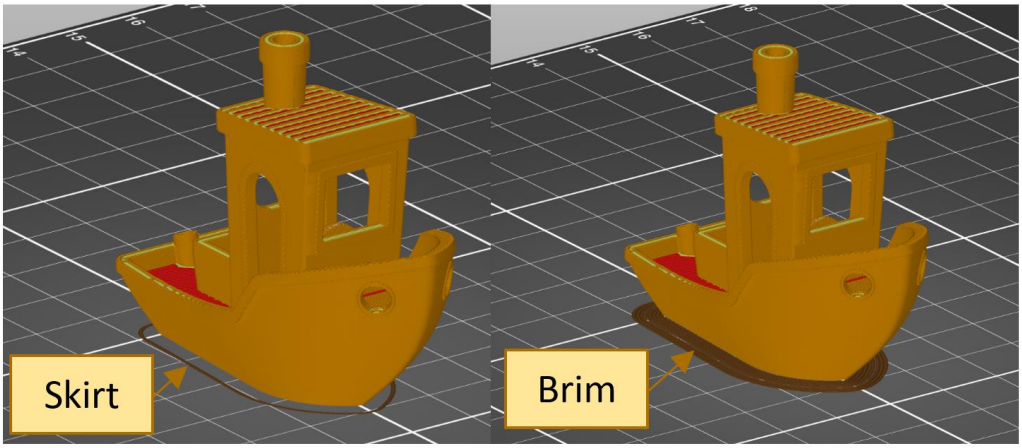

Figure 13 - Left image: part with skirt; Right image: part with brim.

- The use of raft, creating a platform a few layers higher where the part to be produced will be printed, as shown in Figure 14;

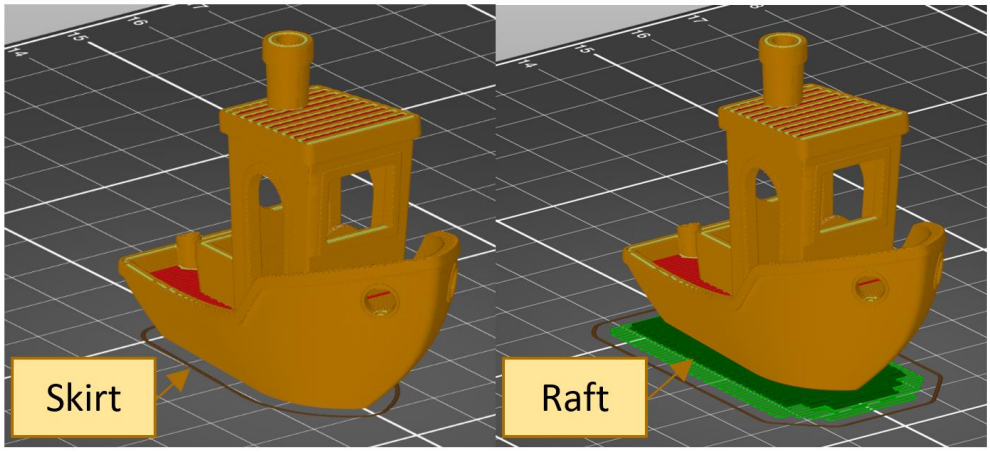

Figure 14 - Left image: part with skirt; Right image: part with raft.

- The first layer should be printed at low speed to allow good adhesion of the filament to the printing surface [11].

Build Orientation

The build orientation of the parts on an FDM printer platform has a significant effect on many characteristics that determine the final quality and cost of manufacturing the part. The

selection of the optimum part deposition orientation is a very important factor as it affects build time, support structure, dimensional accuracy, surface finish, and material consumption. Determining the optimum part deposition orientation is a difficult and time-consuming task as several conflicting objectives such as part surface finish and build time must be considered [11].

The anisotropy effect is much present in the FDM process given its layer construction mode. For this fact, the correct position of the parts in the slicing software is important when optimal mechanical properties need to be achieved. Tensile strength is better when the load is applied perpendicularly to the direction of bead deposition [9]. Figure 15 presents an example that illustrates the direction of layer construction and the direction of stress application.

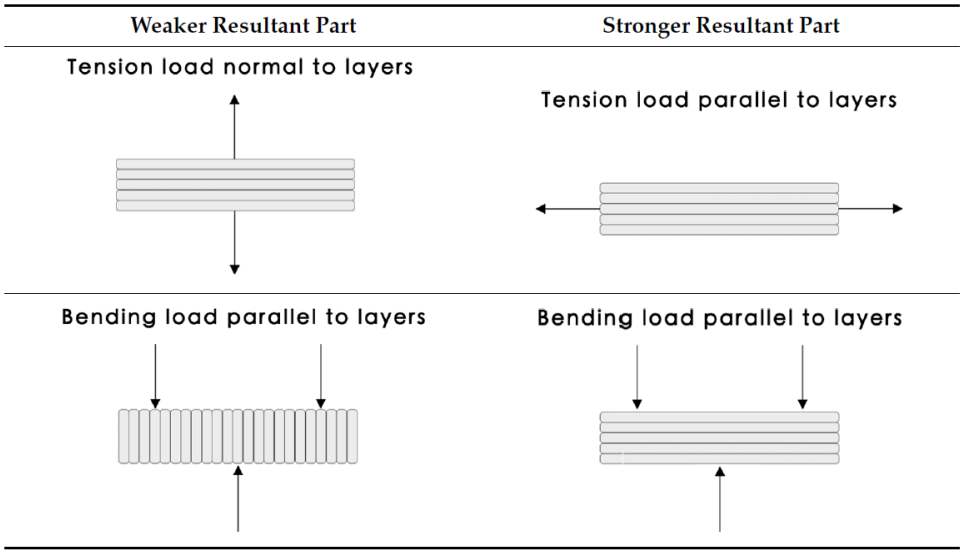

Figure 15 - Direction of construction of the layers and direction of application of tension [9].

Extrusion mechanism

The extruder is responsible for the extrusion of the filament. The extrusion of the filament occurs because the extruder has toothed wheels where the filament passes, which are driven by a motor, thus placing the filament against the heated nozzle. Failures in the extrusion mechanism may occur when the set of toothed wheels responsible for pulling the material are not properly spaced. This failure can be observed when there are small gaps in the deposition of the filament [11]. The solution to this problem is to adjust the distance between these gears in order to improve the material extrusion.

Clogging of the heated nozzle can also cause problems during printing. Nozzle clogging can be caused by contamination of the filament, use of lower extrusion temperatures than those recommended by the material manufacturer, and also by other causes. In the case of using materials reinforced with fibers, the nozzle may be clogged by these fibers if the diameter of the nozzle is 0,4 mm or less. In this case, the solution is to use nozzles with a diameter greater than 0,6 mm [11].

Filament quality

Some filament-related problems may be confused with software-related problems. The fact that filament is very sensitive to environmental factors may mislead the user when correcting problems, which may arise during the printing of a part.

The quality of the filament is a very important point when it is necessary to obtain a good quality part and a stable process. In this case, it must be taken into account if the diameter of the filament is under the dimensional tolerances provided by the manufacturer. A filament with a diameter smaller than that specified by the manufacturer can lead to poor interlayer adhesion, while a larger diameter can cause excessive material flow.

From another perspective, the filament should be stored in a clean, airtight bag or sealed plastic box. It is necessary to ensure that there is no deposition of particles on the filament, as these particles, when the filament is used, will be carried to the heating nozzle and may cause the failure of the material extrusion. One way to avoid this is to use a sponge filter for the filament, as demonstrated in Figure 16.

Figure 16 - Filament cleaner [11].

There are problems caused by the filament that can be confused with parameterization problems, in this case, the presence of moisture in the polymeric material. The polymers used in the manufacture of printed parts are sensitive to environmental factors such as humidity. They can absorb a certain amount of moisture when exposed to humid environments. One way to observe that the filament has moisture is, at the time of extrusion, when small bubbles occur in the molten filament or when hissing sounds appear. When this pattern occurs, it is best to stop printing and remove the filament. Continuing printing the part may result in poor final quality of the part. The filament with moisture can be used after being placed in an airtight bag with some silica bags to absorb the moisture [11].

Oozing

Oozing or stringing are the names given to the small polymeric strands that are formed when the extruder nozzle moves without extrusion occurring (as observed in Figure 17).

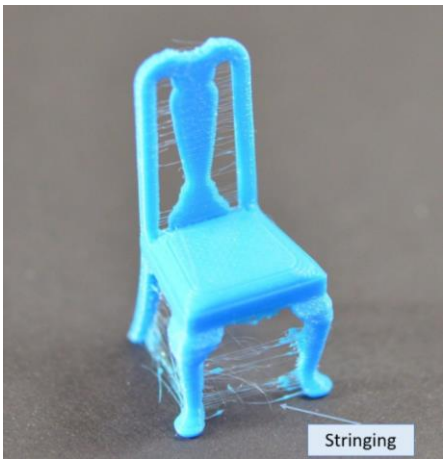

Figure 17 - Printed part with stringing [22].

Oozing mostly occurs when the nozzle temperature is higher than the raw material allows, when the wrong retraction distances are used, low material ratios are reached, or when long extrusion runs occur without extrusion. Oozing can be minimized by gradually reducing the nozzle temperature until the material drag effect reduces to a small amount. Another way to control the oozing effect is to use different retraction and retraction speed values in the slicer program.

Shrinkage is the counter-movement to the extrusion of the filament, performed by the pull motor. The retraction of the material occurs when selected in the CAM program and is requested when there is the movement of the extrusion head without material debt, the value of this distance can also be set in the software. The retraction value, usually in millimeters, corresponds to the distance that the material is pulled in the opposite direction of the extrusion. The value of the speed at which the material is retracted can also be set, as well as the elevation of the Z-axis immediately before the retraction occurs [11].

2.3. **Polymeric material drying**

Most plastics tend to absorb moisture present in their surroundings. This is a reality with plastics in any form, whether as a filament before processing or already in the finished product. These plastics are called hygroscopic or hydrophilic plastics. Plastics that do not absorb moisture are called hydrophobic plastics. Nylons are common examples of hygroscopic plastics. Nylon parts absorb moisture and change the dimensions of the part produced, depending on the amount of moisture absorbed. As a nylon garment absorbs moisture, it can

increase its volume, causing its dimensions to increase beyond its specific required limits. Although moisture absorption is unavoidable in the final piece, excess moisture can be removed from the plastic resin to an acceptable level before being processed [23].

All plastic has a maximum acceptable moisture level, and above such threshold, problems can occur in processing. Table 2 depicts the list of maximum moisture values for some of the materials used in 3D printing [23].

Table 2 - Recommended maximum moisture content for unloaded materials [23].

Polymer name	Acronym	Maximum humidity value [%]
Polylactic acid	PLA	0.010 – 0.032
Acrylonitrile-butadiene-styrene	ABS	0.010 – 0.15
Acrylic styrene acrylonitrile	ASA	0.038 – 0.10
Polymethylmethacrylate	PMMA	0.097 – 0.10
Polyamide 6	PA 6	0.095 – 0.20
Polycarbonate	PC	0.019 – 0.020
Polyethylene terephthalate	PET	0.0030 – 0.20
High impact polystyrene	HIPS	0.1
Thermoplastic elastomer	TPE	0.010 – 0.062
Thermoplastic polyurethane	TPU	0.020 – 0.070

2.4. **Aim of the work**

This work aims to study the impact of pre-dehumidification of polymeric materials such as PLA and PETG used in the FDM process, both on the visual aspect and the mechanical performance of parts produced with and without drying the filament before the extrusion process. Another important analysis is to verify the energy costs involved in the global process. For this, parts will be manufactured with different dehumidification times to be subsequently evaluated visually and mechanically.

3. Materials and methods

3.1. Materials

In the dissertation experiments, two different types of materials for printing the parts, PLA and PETG were used, which are widely used in the FDM process.

3.1.1. PLA filament

Poly-lactic acid (PLA) is a biodegradable thermoplastic polymer due to renewable resources, like sugarcane and corn starch. The dimensional stability, the low price comparingly to other materials used in FDM, and the ease of process make this material user-friendly to introduce this kind of deposition process. PLA is a filament with the best availability and the most attractive cost vs. mechanical properties ratio [24]. The commercial PLA can be various, ranging from soft, elastic materials to stiff, high-strength materials, reinforced, according to different parameters, such as crystallinity, polymer structure, molecular weight, material formulation, and orientation.

Crystallinity is an important characteristic affecting the mechanical properties of PLA, as can be seen the structure-property relationship in Figure 18.

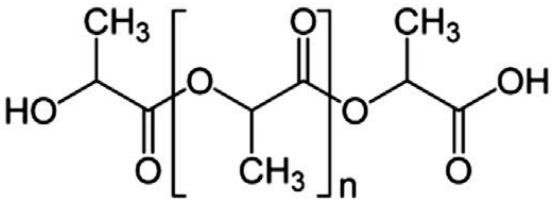

Figure 18 - PLA structure [2].

PLA is a polar polymer, it acts as a hydrolysis process in relation to microorganisms or tissue/organ assimilation [2].

The PLA used has high-quality characteristics, conferred by being an Ingeo 3D870 [25]. This material was designed to provide better heat resistance and high impact resistance to the

3D-printed parts. This formulated grade achieves thermal and mechanical properties similar to Acrylonitrile Butadiene Styrene (ABS). This material also provides excellent printability with precise detail, good adhesion, less warping, and low odor [26]. In Table 3 the physical properties of Ingeo 3D870 are highlighted.

Table 3 - Physical properties for Ingeo 3D870 [26].

Physical properties	Typical Value	ASTM Method
Specific Gravity [g/cc]	1.22	D792
Melt Flow Rate, g/10 min [210ºC/2.16 kg]	9-15	D1238
Peak Melt Temperature [ºC]	165-180	D3418
Glass Transition Temperature [ºC]	55-60	D3418

The mechanical properties of this material are shown in Table 4.

Table 4 - Mechanical properties for Ingeo 3D870 [26].

Mechanical properties	XY Axis	YX Axis	ZX Axis	ASTM Method
Tensile strength [MPa]	40	32	24	D638
Tensile modulus [MPa]	2.865	2.447	2.477	D638
Flexural strength [MPa]	73	49	46	D790
Flexural modulus [MPa]	2.414	1.979	2.352	D790

The temperature profiles recommended by the supplier are shown in Table 5.

Table 5 - Processing temperature profile for Ingeo 3D870 [26].

Processing temperature profile	Metric
Melt temperature	210 ºC
3D printing temperature	190 – 230 ºC
Annealing temperature	110 – 120 ºC
Print bed temperature	None needed (or 50 – 70 ºC if applicable)

The manufacturer's recommended drying temperature for the material is 50 °C for 8 hours.

3.1.2. **PETG filament**

Polyethylene terephthalate (PET) is widely used as synthetic fibers, packaging films, bottles for beverage and food, and engineering plastic components, because of its excellent thermal and mechanical properties, high chemical resistance, and low gas permeability. The PETG has increasing importance in 3D printing, due to its properties such as high impact resistance, high chemical resistance, UV resistance, durability, flexibility, weather resistance, low moisture absorption, recyclability, and does not produce fumes during printing.

The chemical structure of PETG copolyesters, Figure 19, results from the synthesis of terephthalic acid (TPA), ethylene glycol (EG), and 1,4-cyclohexanedimethanol (CHDM) [27].

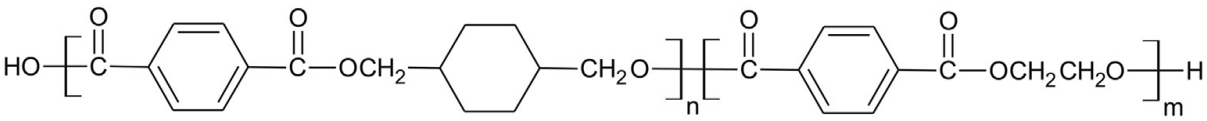

Figure 19 - Chemical structure of the PETG copolyesters [27].

The PETG used is a Prusa Polymers material, called Prusament PETG, and is a very strong material with good heat resistance. Its use is universal but especially suitable for parts for both indoor and outdoor use. PETG has almost no warping. Compared to PLA, it is more heat resistant, more flexible, and less brittle [28]. In Table 6 the physical properties of Prusament PETG are indicated [28].

Table 6 - Physical properties for PETG [28].

Physical properties	Typical Value	Method
Specific Gravity [g/cc]	1.27	ISO 1183
Moisture Absorption 24 hours [%](1)	0.2	Prusa Polymers
Moisture Absorption 7 days [%](1)	0.3	Prusa Polymers
Moisture Absorption 4 weeks [%](1)	0.3	Prusa Polymers
Tensile Yield Strength Filament [MPa]	46 ± 1	ISO 527

(1) 30 ºC; humidity 30%

The mechanical properties of this material are shown in Table 7.

Table 7 - Mechanical properties for PETG [28].

Mechanical properties / Print direction	Horizontal	Vertical X, Y-Axis	Vertical Z-Axis	Method
Tensile Yield Strength [MPa]	47 ± 2	50 ± 1	30 ± 5	ISO 527-1
Tensile Modulus [GPa]	1.5 ± 0.1	1.5 ± 0.1	1.4 ± 0.1	ISO 527-1
Elongation at Yield Point [%]	5.1 ± 0.1	5.1 ± 0.1	2.5 ± 0.5	ISO 527-1

The temperature profiles recommended by the supplier are shown in Table 8.

Table 8 - Processing temperature profile for PETG [28].

Processing temperature profile	Metric
Nozzle Temperature [ºC]	250 ± 10
Heatbed Temperature [ºC]	80 ± 10
Print Speed [mm/s]	Up to 200

The manufacturer's recommended drying temperature for the material is 60 °C for 4 - 8 hours.

3.2. **Methods**

3.2.1. **Apparatus**

Filament Dryer: PrintDry Filament Dryer Pro 2

The PrintDry Filament Dryer Pro is a device designed to dry polymeric filament by heating it to a pre-defined temperature, as illustrated in Figure 20 [19].

Figure 20 - Filament dryer [19].

This device allows 5 temperatures to be set: 35 ºC, 45 ºC, 55 ºC, 65 ºC, and 75 ºC. The maximum drying time of the device can be up to 48 hours continuously, after which it switches off automatically. The double wall allows an efficiency increase during the dehumidification of the contents. This equipment is capable of dehumidifying 2 reels of filament simultaneously, with a maximum diameter of 200 mm each. The maximum consumption of the equipment can reach 245 Wh [19]. The small side openings allow the filament to circulate from inside the dehumidifier chamber directly to the 3D printer [19].

3D Printer: Prusa i3 MK3s

The 3D printer used was a Prusa i3 MK3s, a Moving Bed type printer as mentioned earlier in subsection 2.2.1, and can be depicted in Figure 21.

Figure 21 - Prusa i3 MK3s [29].

The printer used has outside dimensions of 500 x 550 x 400 [mm] and weighs 7 kg. This printer has a build volume of 250 x 210 x 210 [mm], uses a 1.75 mm diameter filament, and can achieve a layer accuracy of 0.05 mm. The maximum consumption of the equipment can reach 200 Wh. The maximum temperature of the extruder hot block can reach 300 °C and the heated base can reach 120 °C, thus enabling the use of a wide range of thermoplastics such as PETG, ASA, ABS, PC, CPE, PVA/BVOH, PVB, HIPS, PP, Flex, nGen, Nylon and carbon filled materials, wood and other fillers.

The consumption of the equipment is 80 Wh for the settings used in PLA and 120 Wh for the settings used in ABS [29].

Arduino project: Arduino Mega 2560 + DHT22 sensor

The Arduino Mega 2560, presented in Figure 22, is a microcontroller board based on the ATmega2560 microcontroller [30]. This board contains 54 digital input/output pins, a 16 MHz crystal oscillator, 16 analog inputs, 4 UARTs (hardware serial ports), a USB connection, an ICSP (In-Circuit Serial Programming) header, a power jack, and a reset button [31].

Figure 22 - Arduino Mega2560 [32].

The DHT-22 sensor, presented in Figure 23, is a digital sensor that is used to measure the temperature and humidity of the surrounding air. This sensor uses capacitive humidity sensors and thermistors to measure the ambient temperature, connected to single-chip 8-bit computers and converted to digital signals on the data pin [33].

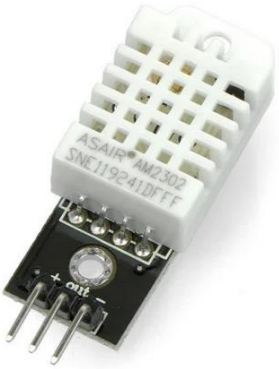

Figure 23 - DHT-22 sensor [34].

The way this sensor measures humidity is to use two electrodes to hold the substrate moisture between the two electrodes. The change in the conductivity of the substrate or the resistance between the two electrodes increases the moisture values obtained by the sensor. The sensor's integrated circuit measures and processes the data collected by the sensor and makes it ready to be read by the microcontroller [33].

Smart Wi-Fi Plug: Shelly Plug

The Shelly Plug, presented in Figure 24, allows to remotely control any device plugged into it. This socket contains a mechanism and an accurate power measurement system.

Figure 24 - Shelly Plug [35].

It contains a local and remote control system, via wi-fi from a mobile phone, computer, automation system, or other [35].

Universal testing machine: Zwick Roell Z100

According to standard D638, the test machine shall be of the constant rate-of-crosshead-movement type, containing a fixed member with one grip and a moving member with a second grip where the grips shall be of the fixed or self-aligning type. The drive mechanism can transmit a uniform and controlled speed to the moving member relative to the stationary member. The load indicating mechanism shall be free from inertia and shall be suitable for showing the total tensile load applied to the test specimen [3].

In compliance with standard D638, the Mechanical Department of the Polytechnic of Leiria has a universal testing machine Zwick Roell Z100, presented in Figure 25, and can perform tests up to 100 kN load. The maximum height of the test area is 1360 mm and the width is 640 mm. The crosshead speed can be from 0.001 to 200 mm/min [36].

Figure 25 - Zwick Roell Z100 [36].

The testing machine contained a dedicated computer in order to record all the data obtained during the tests.

Analytical balance: Mettler Toledo AG204

The Mettler Toledo AG204 analytical balance is a user-friendly balance due to its motorized internal calibration by means of a standard weight and by external calibration with 40 g, 100 g, and 200 g weight (Figure 26). [37]

Figure 26 - Analytical balance Mettler Toledo AG204 [37].

This scale contains an operation menu with functions such as adaptability to weighing conditions, select calibration function, weighing process adapter, repeatability, automatic zero

correction, primary and alternative weighing units, and interface output parameters. Some features of this scale are 0.1 mg reading capacity, maximum capacity of 210 g, linearity of +- 0.2 mg, and a stabilization time of 3 seconds.

3.2.2. **Aesthetic test method**

The geometry of the piece defined for the experiments was a piece containing two quadrangular pyramids and a cylinder, arranged at different distances and resting on a base, as illustrated in Figure 27.

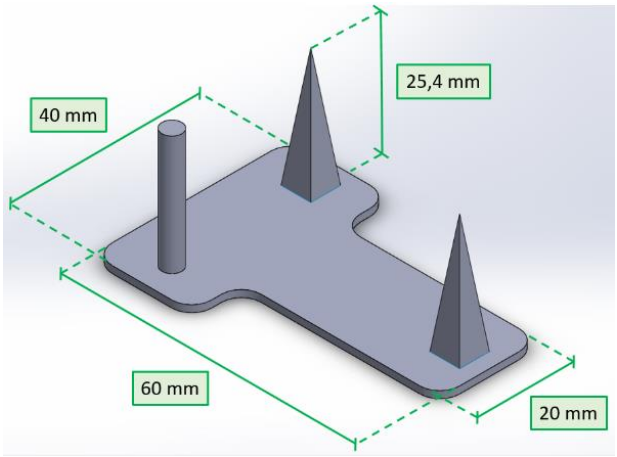

Figure 27 - Part geometry used for tests.

The cylinder geometry and the pyramid-shaped geometries were chosen because they enhance the appearance of the defect, and material dragging, given the fact that they contain many paths without material flow.

3.2.3. **Mechanical test method**

The ASTM D638 standard is defined as a testing method to determine the tensile strength of both reinforced and non-reinforced plastics. This protocol is performed on standard dumbbell-shaped test specimens and under defined conditions of pretreatment, temperature, humidity, and testing machine speed. This test measures how its properties change under extreme tensions, to demonstrate the resistance of plastic to tensile forces [3] [38].

For the type of test specimens intended for this study, standard D638 divides them into 3 categories [3]:

- rigid and semi-rigid plastics;
- non-rigid plastics;
- reinforced composites.

The test specimens to be used for the tensile tests shall meet certain dimensional requirements. ASTM D638-10 provides five dimensions of test specimens, as depicted in Figure 28, for determining the tensile properties of plastics [4].

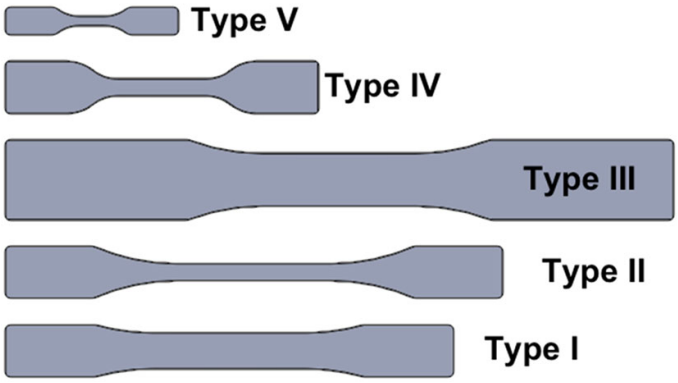

Figure 28 - Illustration of the five tensile test specimens [38].

In Table 9 the dimensions of the five test specimen types are detailed.

Table 9 - ASTM D638 Specimen dimensions [3].

Dimensions [mm]	Type I	Type II	Type III	Type IV	Type V
W - Width of the narrow section	13	6	19	6	3.18
L - Length of the narrow section	57	57	57	33	9.53
WO - Width overall	19	19	29	19	9.53
LO - Length overall	165	183	246	115	63.5
G - Gage length	50	50	50	25	7.62
D - Distance between grips	115	135	115	65	25.4
R - Radius of fillet	76	76	76	14	12.7
T - Thickness	3.2	3.2	3.2	3.2	3.2

Figure 29 shows all the dimensions of the specimen highlighted in the previous table for the test specimens for type I, type II, type III, type IV, and type V.

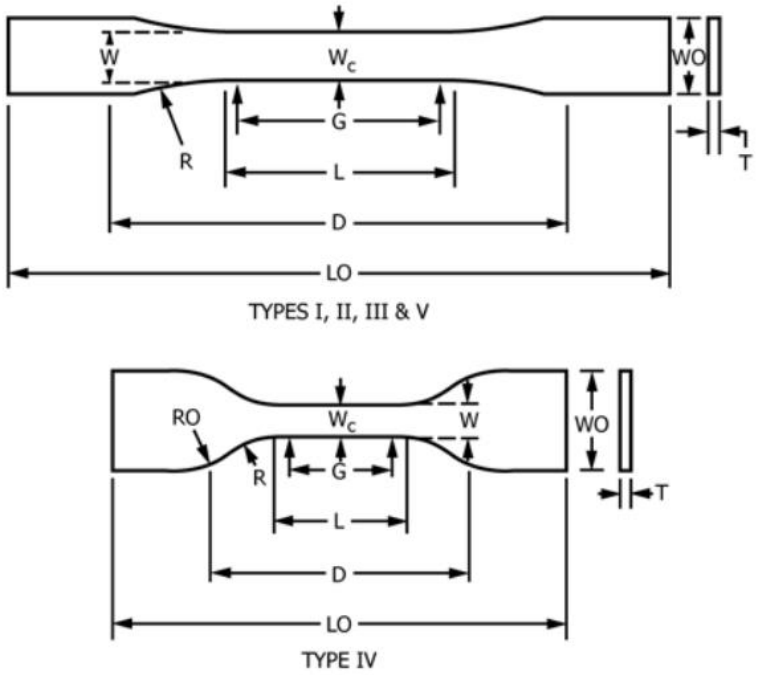

Figure 29 - Dimensions of the types of specimen according to the standard D638 [3].

In the D638 standard, type IV is referred to as the test specimen commonly used when a direct comparison between materials in different stiffness cases is required and for this reason, it was the type of specimen used in the mechanical tests performed in this work. This was the only feature used in the selection of the test specimen because it is not clear in the standard which is the most suitable test specimen to use for FDM manufactured parts [3].

Considering that there are few specific test standards for polymer-based AM technologies, it was determined to perform tensile tests. The tensile strength of a part obtained through additive manufacturing by the FDM process may generate different tensile strengths by the form it is obtained. This is due to the anisotropic nature of this additive manufacturing technique since the anisotropy is related to the orientation of the specimen construction, (ZXY or XYZ) [4], as illustrated in Figure 30.

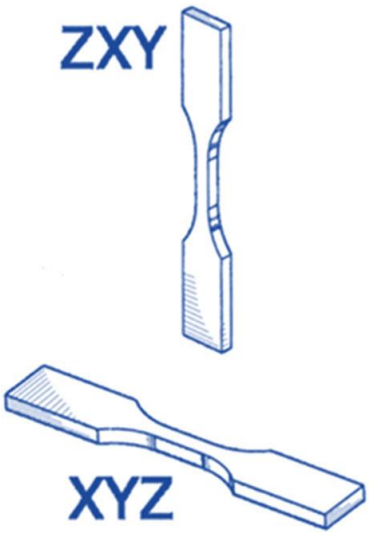

Figure 30 - Illustration of the type of build ZXY and XYZ [3].

Normally, in the FDM process, the specimens produced in the ZXY object tend to have lower tensile strength values when compared to equivalent specimens produced in the XYZ object [4].

4. Experiments

4.1. **Arduino setup**

To carry out the tests, with greater accuracy, there was the need to create a simple project with the use of an Arduino and sensors for measuring temperature and humidity (DHT-22), because the dehumidifier doesn't provide the actual reading of the temperature inside the chamber, only allows the introduction of setup values for temperature. For the selection of the sensors, low cost sensors were chosen, with sufficient numerical resolution for the purpose.

The DHT-22 sensors were placed in 4 different locations to collect accurate temperature and humidity data, three inside the drying chamber (as can be observed in Figure 31) and one outside the drying chamber to collect room data (as depicted in Figure 32).

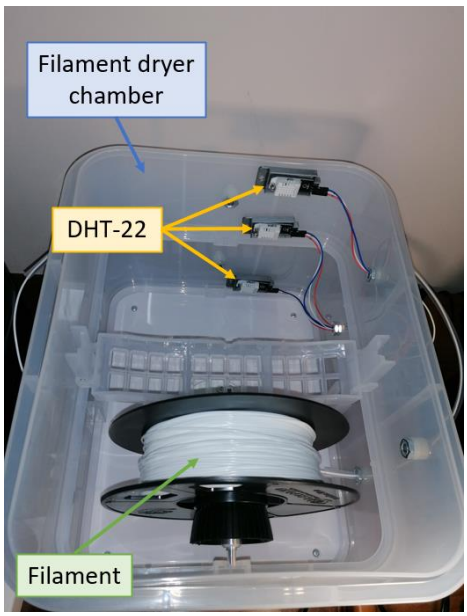

Figure 31 - Drying chamber setup.

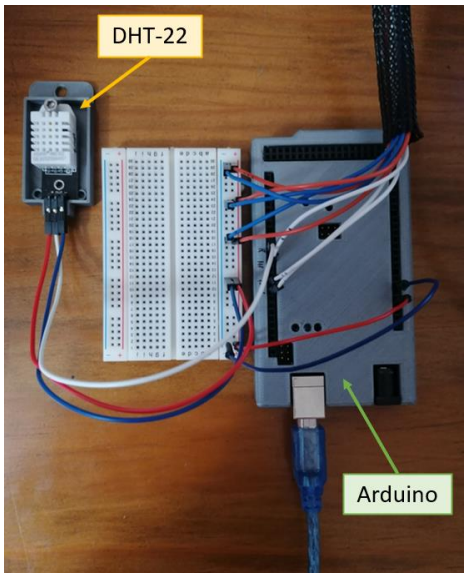

Figure 32 - Arduino and sensor outside the chamber.

Inside the dehumidifier, the sensors were placed aligned and on top of each other (as depicted in Figure 33), to register the different temperatures inside the chamber, so that in the end it was possible to calculate the real average temperature.

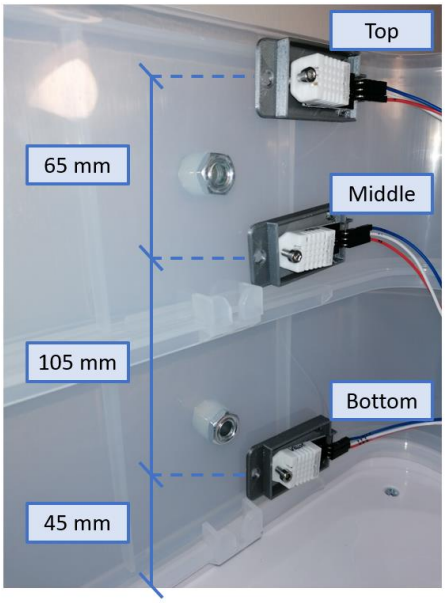

Figure 33 - Location of the sensors inside the chamber.

In order to be more clear, in Figure 34 the connections of the sensors to the Arduino.

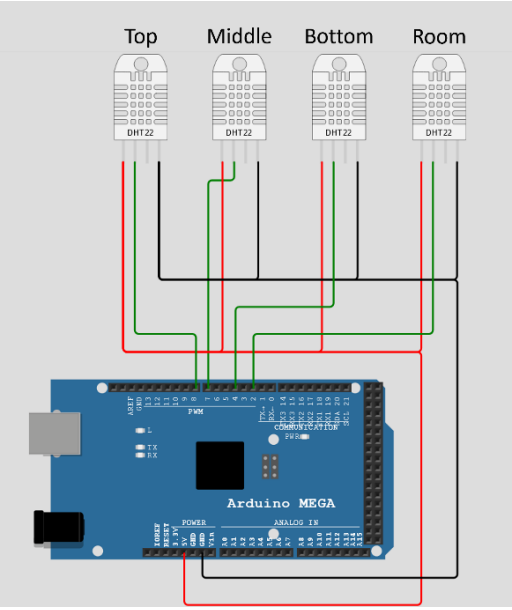

Figure 34 Arduino and sensors connections.

The colored lines, indicated in the previous figure, represent the connections made in the system and have different meanings. In the case of the black lines, they refer to the ground circuit, 0V, and connect to the fourth pin of each sensor. The red line refers to the power supply of the sensors, in this case, 5V. The green lines connect to the digital inputs, numbered respectively.

4.2. **Aesthetic tests**

The experimental procedure aims to demonstrate the comparison at a visual level of parts that were built without the filament being dehumidified and parts whose filament was dehumidified for 3 hours and 6 hours.

A moving bed printer with a direct drive and a 0.6 mm diameter nozzle was used to manufacture the parts. An appropriate dehumidifier was used to remove moisture from the filaments, as shown in subsection 3.2.1, in the filament dryer explanation.

4.2.1. **PLA filament**

PLA (Poly-lactic acid) is a biodegradable thermoplastic typically obtained from corn or potatoes. PLA filament is generally extruded using low temperatures, between 160 °C to 220 °C, and can be printed without temperature on the heating bed [12].

Table 10 presents the parameters used to print the PLA samples.

Table 10 - Parameters used to produce PLA parts.

Parameter Type	Metric	Value
Layers and perimeters	Layer height	0.2 mm
	First layer height	0.2 mm
	Shell thickness top	0.9 mm
	Shell thickness bottom	0.6 mm
Infill	Fill density	100%
	Fill pattern	Rectilinear
Speed	Perimeters	45 mm/s
	Infill	70 mm/s
	Top solid infill	45 mm/s
	Bridges	25 mm/s
Extruder	Nozzle diameter	0.6 mm
	Retraction length	0.8 mm
	Retraction lift Z	0.4 mm
Filament	Diameter	1.75 mm
	Nozzle temperature	210 °C
	Bed temperature	60 °C

Analysis of the part without material pre-processing

The filament used to print the piece was exposed to ambient temperature and humidity. For these conditions, 19 °C and 63.4% humidity were recorded at the time of printing the piece. At the end of printing, the piece has some defects, such as material dragging in the transition of vertical geometries, as shown in Figure 35.

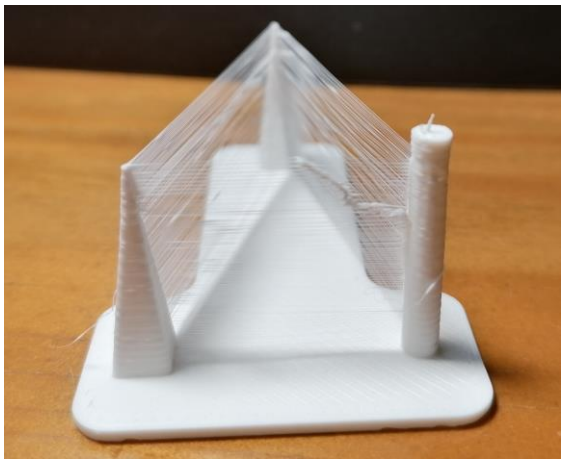

Figure 35 - Piece printed in PLA with the filament without being dehumidified.

In addition to the defect mentioned above, the part had some flaws in filling the layers, as illustrated in Figure 36.

Figure 36 - Printed part base without filament dehumidification.

The defects shown are visible throughout the part, both the involuntary extrusion of material and the incomplete ones visible in the first layer.

Analysis of the printed piece with 3 hours of material dehumidification

The filament used in this test was properly conditioned in an appropriate dehumidifier for the purpose, at a setup temperature of 55 °C for 3 hours. During the printing of the part, the values were collected and the average values were recorded in Table 11.

Table 11 – Average values collected for 55 °C setup for 3 hours.

	Temperature [°C]	Moisture [%]
Top	49.7	15.5
Center	49	17
Bottom	55.1	15.2
Exterior	21.6	53.3

Visually, the piece obtained shows a significant reduction in the involuntarily extruded material, as can be seen from Figure 37.

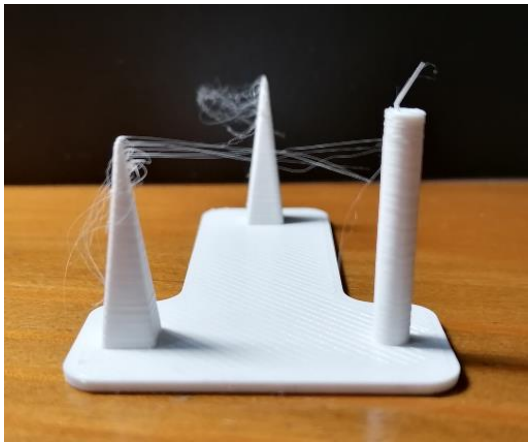

Figure 37 - Printed part after 3 hours of material dehumidification.

The base of the part also shows a better result after having been printed with the dehumidified material as described above, a result that can be seen in Figure 38.

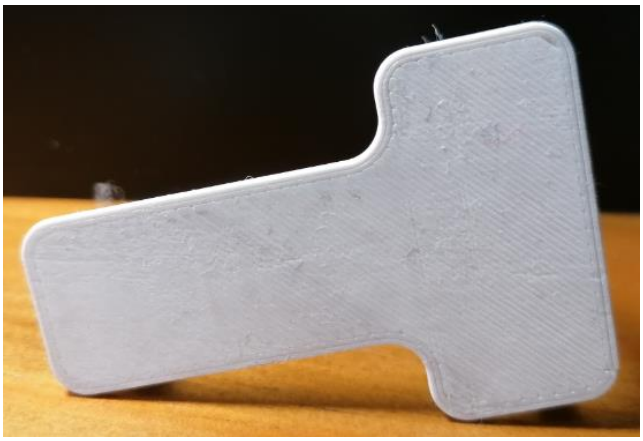

Figure 38 - Printed part base after 3 hours of material dehumidification.

Visually, the printed part after dehumidifying the material for 3 hours presents a superior quality to the test of the printed part without the previously dehumidified material.

Printed part analysis with 6 hours of material dehumidification

This test was performed using the same equipment, but this time using a temperature of 55 °C for 6 hours to dehumidify the material. The average values collected by the sensors installed inside the dehumidifier are shown in Table 12.

Table 12 – Average values collected for 55 °C setup for 6 hours.

	Temperature [°C]	Moisture [%]
Top	45.6	16.8
Center	45.7	17.7
Bottom	51.9	15.6
Exterior	19.1	60.2

With the change from 3 hours of material dehumidification to 6 hours, a part very similar to the part printed in the previous test was obtained. The defect is similar and appears in the same areas, as shown in Figure 39.

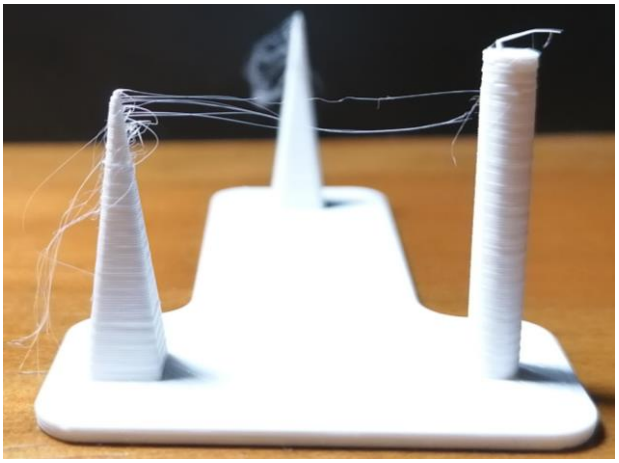

Figure 39 - Printed part after 6 hours of material dehumidification.

The base of the piece presents a result also identical to the one described above, a uniform base without incomplete filling, as can be seen in Figure 40.

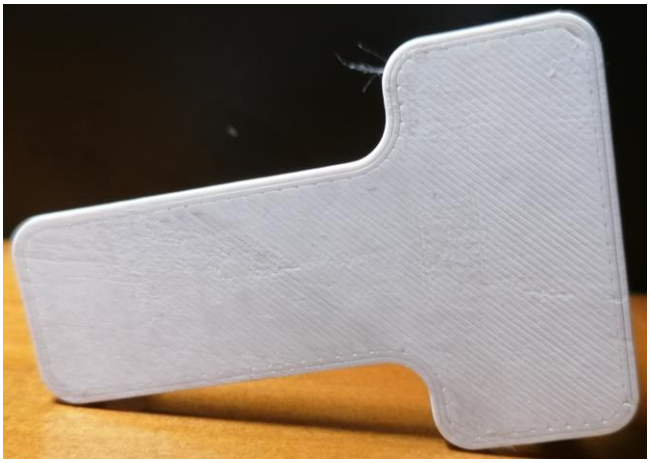

Figure 40 - Printed part base after 6 hours of dehumidification.

The results obtained in the first layer are similar to those obtained in the previous test, with no material defects in the first layer. Without dehumidification it is clear the worst visual result, at 3h the visual appearance of the pieces improves, however at 6h there is no significant improvement.

The graph represented in Figure 41 shows the temperature values inside and outside the material drying equipment. The values inside the chamber were collected using the middle sensor.

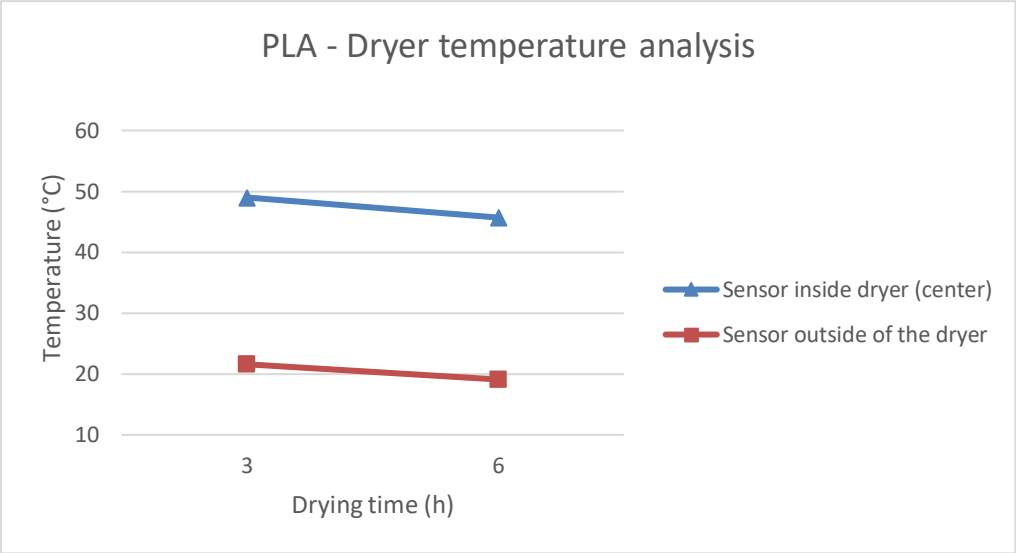

Figure 41 - Graph of the temperature analysis in the dryer for PLA

We can observe that for 3 and 6 hours, the graph obtained from the sensor inside the dryer and the graph obtained from the sensor outside the dryer are similar. This result may indicate the impact of external factors on the equipment since the temperature inside the dryer decreased as the temperature outside the dryer decreased.

The graph represented in Figure 42 depicts the humidity values for the same states, sensor locations, and dehumidification time.

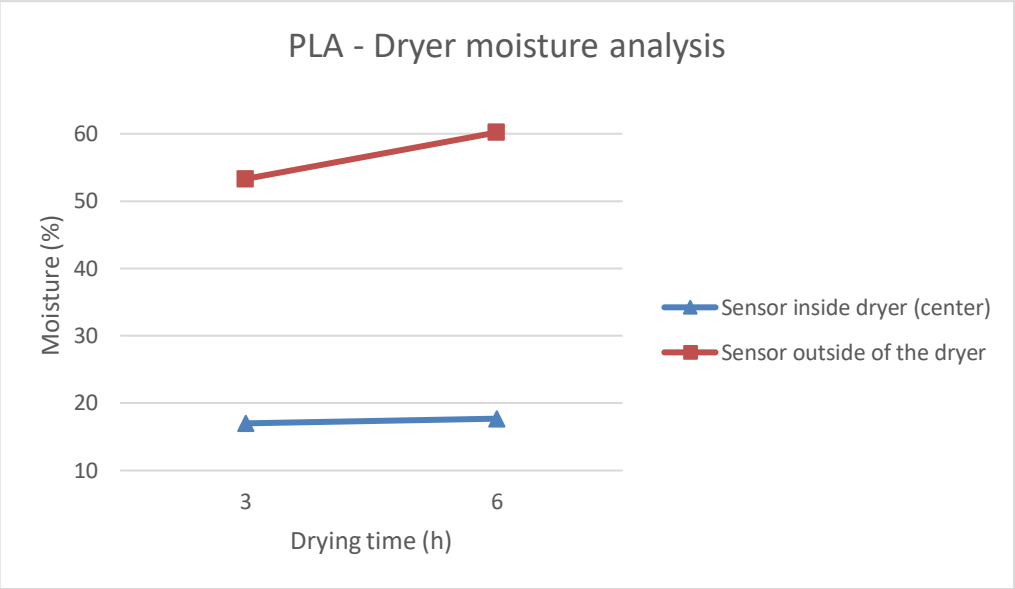

Figure 42 - Graph of the moisture analysis in the dryer for PLA

By analyzing the graph, a change in the humidity values outside the equipment is visible, which also had a slight impact on the humidity percentage recorded inside the dryer. It can be observed that the humidity has a little variation inside the dryer between 3 and 6 hours.

The conclusion drawn after observing the plot is that the equipment during the defined time interval was not able to reduce the moisture level inside, not reducing more than 17%.

4.2.2. **PETG filament**

PETG (Poly Ethylene Terephthalate Glycol) is a thermoplastic with a low warping coefficient, very resistant, not brittle and the adhesion between layers is good [39]. The processing temperature of the parts using PETG was 240 °C in the hot nozzle. The recommended processing temperature for processing this material is 250 ± 10 °C in the hot nozzle, and 90 °C in the heated base, with the recommended temperature being 80 ± 10 °C.

Table 13 presents the parameters used to print the PETG parts.

Table 13 - Parameters used to produce PETG parts.

Parameter Type	Metric	Value
Layers and perimeters	Layer height	0.2 mm
	First layer height	0.2 mm
	Shell thickness top	0.9 mm
	Shell thickness bottom	0.6 mm
Infill	Fill density	100%
	Fill pattern	Rectilinear
Speed	Perimeters	45 mm/s
	Infill	70 mm/s
	Top solid infill	45 mm/s
	Bridges	25 mm/s
Extruder	Nozzle diameter	0.6 mm
	Retraction length	0.8 mm
	Retraction lift Z	0.4 mm
Filament	Diameter	1.75 mm
	Nozzle temperature	210 °C
	Bed temperature	60 °C

Analysis of the part without material pre-processing

Using the same conditions as for the PLA piece experiment, the filament was exposed to room temperature and humidity. For these conditions, 19 °C and 63.4% humidity were recorded at the time of printing the piece. At the end of printing, the piece presents a more pronounced drag in the transitions of the vertical geometries, as can be seen in Figure 43.

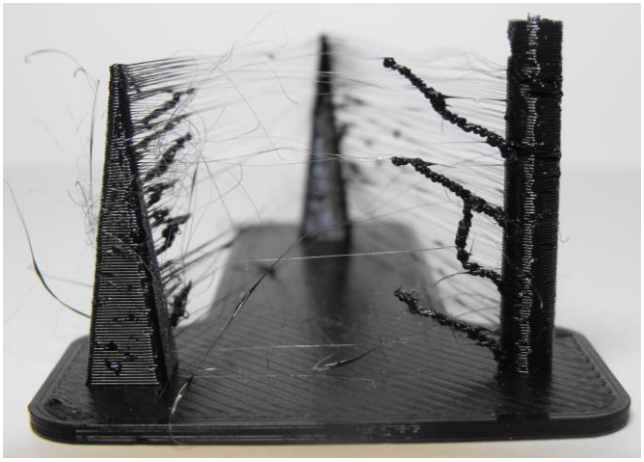

Figure 43 - Part printed in PETG without material dehumidification.

The material imperfections in the piece under analysis are not so visible at the base, compared to the result obtained with PLA, but they are more evident in the construction of the layers, as can be seen in Figure 44.

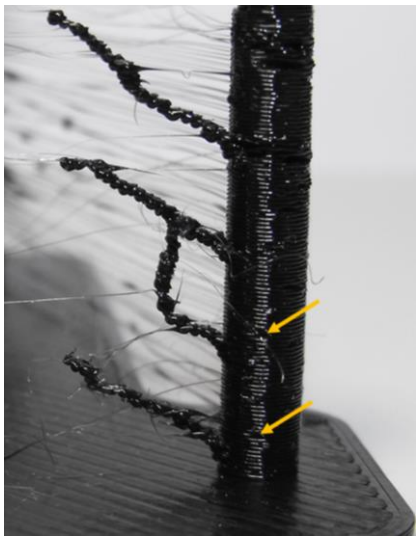

Figure 44 - Part with material flaws in the construction of layers.

In the first layer of the printed part, the material imperfections are not in as much quantity as those that originated in the PLA printing under the same conditions, without material dehumidification, as can be seen in Figure 45.

Figure 45 - Printed part base without material dehumidification.

Part analysis with 3 hours of dehumidification

The filament used in this test was allowed to dehumidify at a temperature of 65 °C for 3 hours. When printing the test piece, the average values obtained by the sensors installed inside the dehumidifier are shown in Table 14.

Table 14 – Average values collected for 65 °C setup and 3 hours.

	Temperature [°C]	Moisture [%]
Top	54.6	13.2
Center	54.4	14.4
Bottom	60.8	13.4
Exterior	19.5	57.5

The results of the printed part, after the material has been submitted to the conditions presented in the previous table, can be seen in Figure 46.

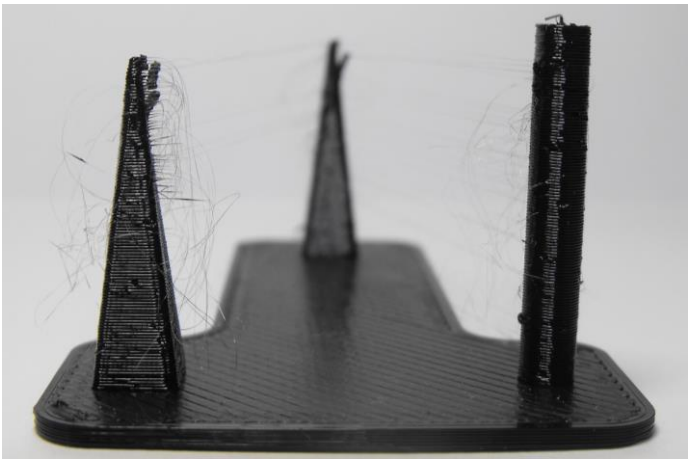

Figure 46 - Printed part after 3 hours of material dehumidification.

After manufacturing the part, the improvements in the object are quite visible. Although it still has defects, the amount of material deposited involuntarily in the transitions between the pyramid shapes and the cylinder has significantly reduced. In the construction of the layers, it is still possible to verify the appearance of some material imperfections, although of smaller dimensions and in smaller quantities than in the previous case, as can be seen in Figure 47.

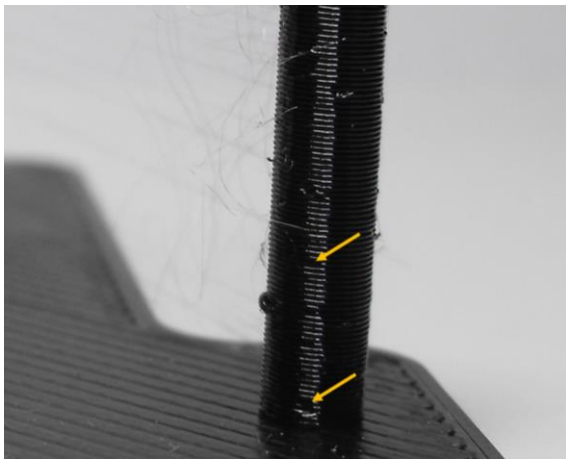

Figure 47 - Part with material flaws in the construction of layers.

The first layer also presents a reduction in imperfections due to a lack of material. The more uniform filling of the first layer can be seen in Figure 48.

Figure 48 - First layer after 3 hours of material dehumidification.

Part analysis with 6 hours of dehumidification

The filament used in this test was placed in the dehumidifier at a temperature of 65 °C for 6 hours. During the printing of the part, the average values obtained by the sensors installed inside the dehumidifier are shown in Table 15.

Table 15 – Average values collected for 65 °C setup and 6 hours.

	Temperature [°C]	Moisture [%]
Top	52.3	14
Center	52	15.1
Bottom	59.6	13.6
Exterior	20.5	53.9

In table 15 it is possible to observe that in terms of temperature values, these are much lower in the 6-hour test of dehumidification of the material. The humidity values, on the other hand, differ by around 40% from the humidity value collected from outside the equipment. The piece resulting from this test has a more uniform layer construction and less material drag, as can be seen in Figure 49.

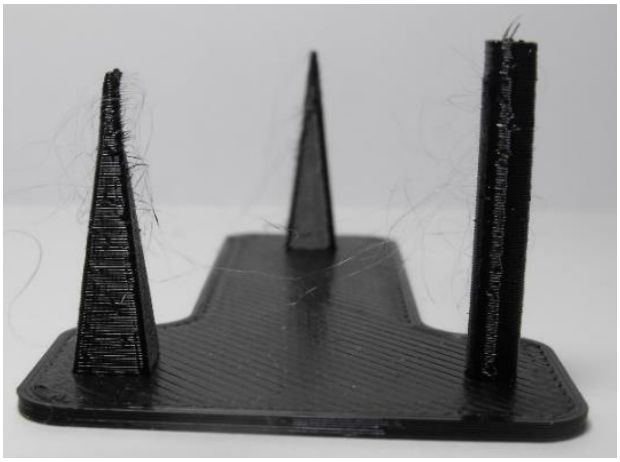

Figure 49 - Printed part after 6 hours of material dehumidification.

Although the results obtained may be significantly better than the previous ones, the defects are still visible. It can be observed in detail, in Figure 50, the defects present in the cylindrical geometry of the printed piece.

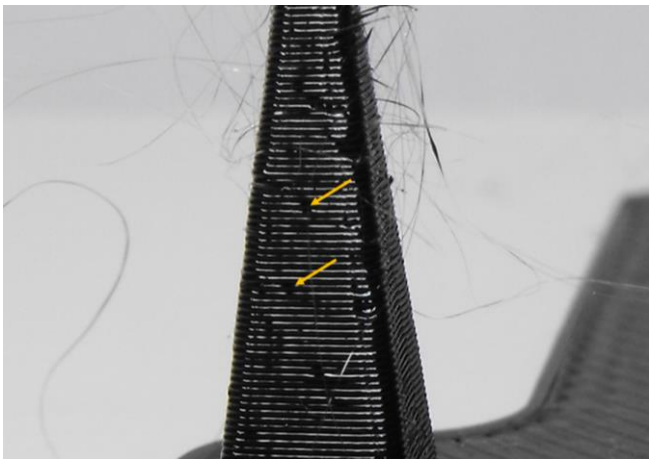

Figure 50 - Lack of material in the part layers.

The first layer of the printed piece has a superior quality to the others, with a uniform filling, and without flaws in its construction. The result of this printing can be seen in Figure 51.

Figure 51 - First layer after 6 hours of material dehumidification.

Without previous material dehumidification, the printed parts show poor visual quality, which improves with 3-hour dehumidification. The 6-hour material dehumidification improves when compared to the 3-hour dehumidification.

Compared to PLA, PETG shows significant improvements at 6 hours of dehumidification while PLA shows such improvements at 3 hours of dehumidification.

Similarly to PLA, a graph was prepared for PETG to analyze the temperature inside and outside the dryer, Figure 52.

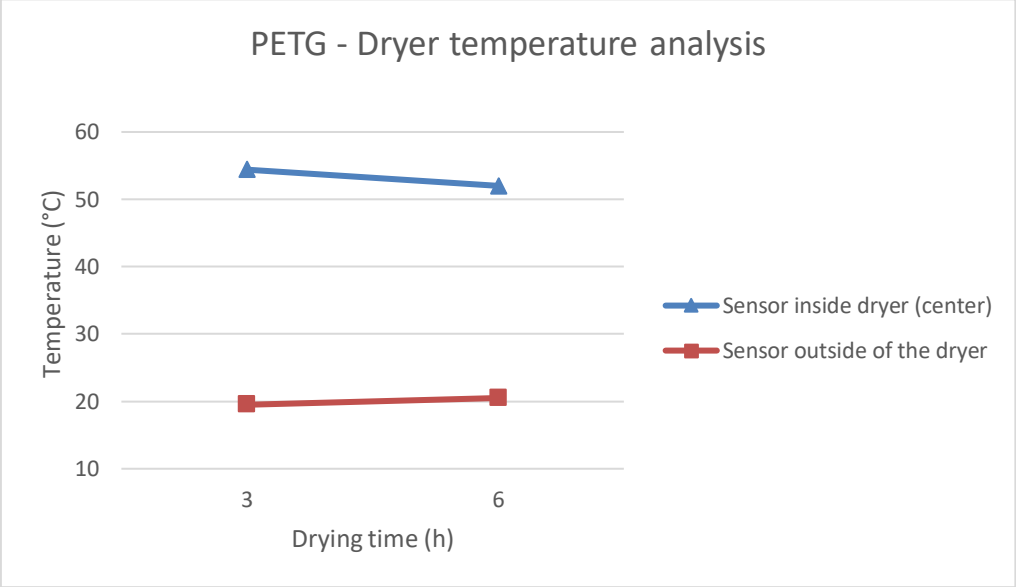

Figure 52 - Graph of the temperature analysis in the dryer for PETG.

Using the plot represented in the previous figure is observed that the graphs obtained by the sensor inside the dryer and the sensor outside the dryer do not follow the same trend, while the temperature outside the dryer rises slightly, the temperature inside the dryer decreases. This scenario may be due to a thermal leakage from the inside of the equipment at the 6 hours experiment.

A graph was also prepared to understand what the percentage moisture values were for PETG, Figure 53.

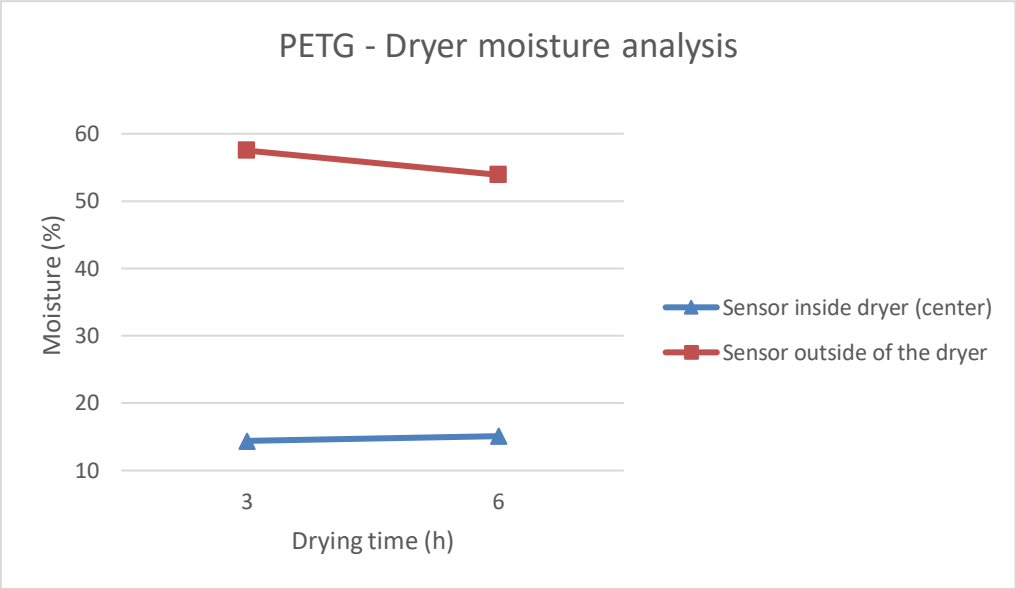

Figure 53 - Graph of the moisture analysis in the dryer for PETG.

Compared with the graph obtained for temperature, it is visible that the humidity graph has the same pattern, decreasing the percentage of humidity outside and slightly increasing the humidity inside.

The percentage of moisture inside the dryer remains between 14% and 15%, which reflects the moisture reduction capacity of the dryer for 6 hours.

The graphs obtained for PETG, when compared to PLA, may indicate a difference in its pattern. This difference may have been caused by a thermal leak from the inside to the outside of the equipment at the time of the aesthetic tests.

4.2.3. **Weight of parts**

The parts analyzed in the aesthetic tests were weighed, as a way to compare the impact of the effect of dehumidification on the amount of material deposited in the fabrication. The weighing values are shown in Table 16.

Table 16 - Weight of parts comparison.

	Parts in PLA [g]	Parts in PETG [g]
0h dehumidification time	3.31	3.51
3h dehumidification time	3.43	3.50
6h dehumidification time	3.44	3.49
CAD software	3.08	3.20
Slicer software	3.76	3.92

For the CAD software and the slicer, the respective densities of the materials were used, 1.22 g/cm^3 for PLA and 1.27 g/cm^3, according to the filament manufacturer's datasheet.

The values simulated by the software are approximate to the values obtained when weighing the pieces. In the weighing of the pieces, the behavior in PLA is different from that of PETG, where PLA tends to increase the mass with the increase of dehumidification time and PETG tends to reduce the mass with the increase of dehumidification time.

4.3. **Tensile tests**

The experimental procedure was aimed at testing fabricated specimens whose material was not dehumidified previously and specimens in which the filament was dehumidified for 6 hours. The real temperature used to dehumidify the materials was 50 °C for PLA and 60 °C for PETG. The average humidity value inside the dehumidified chamber was 21.2% while outside the chamber the humidity value was 65.5%.

A PrintDry Filament Dryer 2.0 filament dehumidifier was used for dehumidification. After this process, the filaments were processed using a Prusa i3 MK3s printer to build test specimens for the tensile test. The processing parameters regarding deposition were similar except for the temperature: for the filament extrusion and the deposition base.

Figure 54 shows the specimens used as well as the main dimensions.

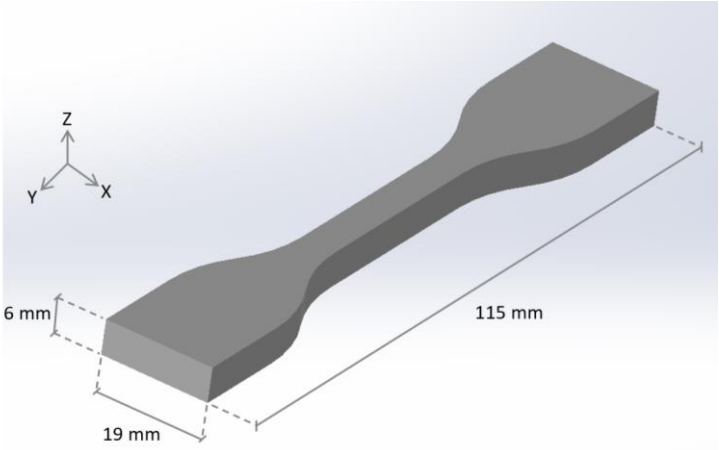

Figure 54 - Main dimensions and print orientation of the part used in the tensile tests.

PLA and PETG test specimens were manufactured using similar process values and building methods except for the temperature of the hot block and the heated printer base.

In Table 17 we have the parameters used to print the PLA samples.

Table 17 - Parameters used to produce PLA specimens.

Parameter Type	Metric	Value
Layers and perimeters	Layer height	0.2 mm
	First layer height	0.2 mm
	Shell thickness top	0.9 mm
	Shell thickness bottom	0.6 mm
Infill	Fill density	100%
	Fill pattern	Rectilinear
Speed	Perimeters	45 mm/s
	Infill	70 mm/s
	Top solid infill	45 mm/s
	Bridges	25 mm/s
Extruder	Nozzle diameter	0.6 mm
	Retraction length	0.8 mm
	Retraction lift Z	0.4 mm
Filament	Diameter	1.75 mm
	Nozzle temperature	210 °C
	Bed temperature	60 °C

In Table 18 we have the parameters used to print the PETG specimens.

Table 18 - Parameters used to produce PETG specimens.

Parameter Type	Metric	Value
Layers and perimeters	Layer height	0.2 mm
	First layer height	0.2 mm
	Shell thickness top	0.9 mm
	Shell thickness bottom	0.6 mm
Infill	Fill density	100%
	Fill pattern	Rectilinear
Speed	Perimeters	45 mm/s
	Infill	70 mm/s
	Top solid infill	45 mm/s
	Bridges	25 mm/s
Extruder	Nozzle diameter	0.6 mm
	Retraction length	0.8 mm
	Retraction lift Z	0.4 mm
Filament	Diameter	1.75 mm
	Nozzle temperature	250 °C
	Bed temperature	80 °C

The fact that the FDM process is a process that causes anisotropy during part construction, the specimens were constructed as illustrated in Figure 55, in order to orient the fibers in the direction of the test movement.

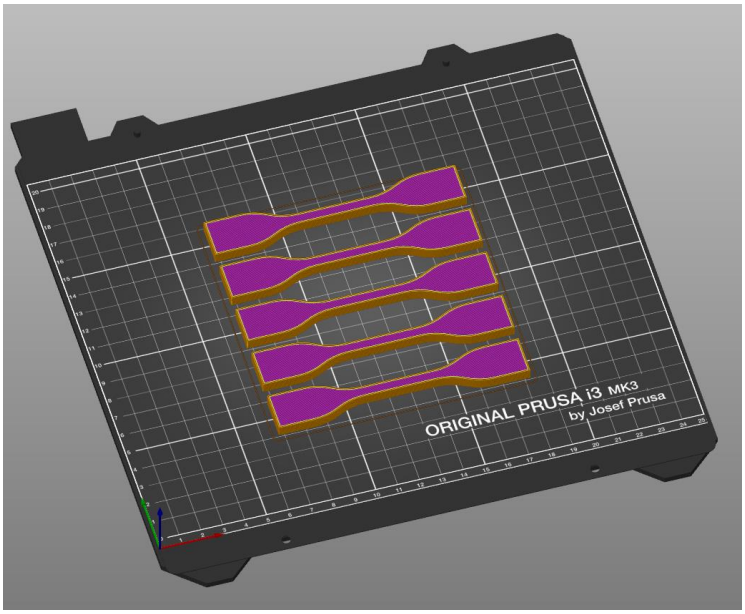

Figure 55 - Specimen construction layout.

The specimens were then subjected to tensile testing at a constant strain rate of 1 mm/min according to ASTM D 638-02. Figure 56 shows the charts referring to the tests performed on the specimens made of PLA and PETG, expressed in stress/strain. It is possible to observe the mechanical behavior curves of the test specimens. For the specimens made of PLA, the mechanical strength is about 2% higher in the specimen whose filament was not previously dehumidified. In the case of PETG, the mechanical behavior is very similar, with the specimens produced with non-dehumidified filament presenting 3% higher mechanical resistance than those produced with dehumidified filament.

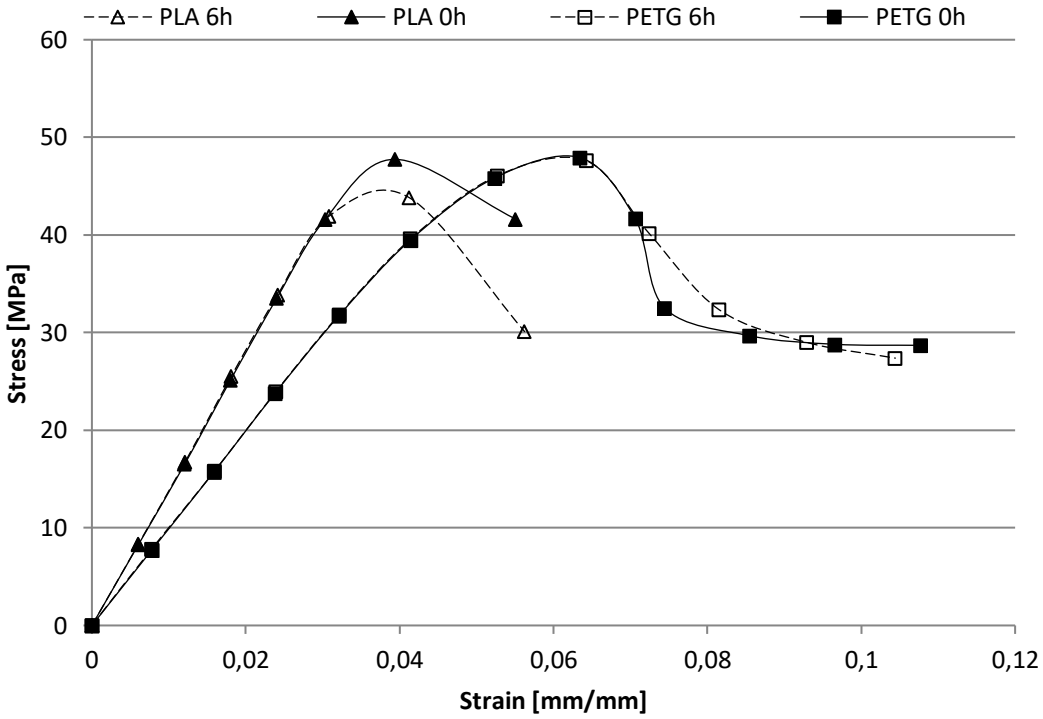

Figure 56 - Evolution of the mechanical behavior of PLA and PETG.

The indication 0h refers to the non-dehumidified filament, the dehumidified specimens have the indication 6h, which means they have been dehumidified for 6 hours.

Table 19 summarises the two mechanical properties evaluated in the tensile test. From the tests performed and data obtained, it can be seen that for both materials tested, there is a slight decrease in mechanical strength after dehumidification.

Table 19 - Results obtained in the tensile strength tests.

Material	Dehumidification time [h]	Tensile Strength [MPa]	Modulus of longitudinal elasticity [GPa]
PLA	0	47.47	1.462
	6	46.53	1.405
PETG	0	49.46	1.003
	6	48.12	1.005

After analyzing the previous table, a relationship was found between the parts produced with dehumidified material and the parts produced with non-dehumidified material, both in PLA and PETG. Having in focus the mechanical resistance of the material, the demand is the manufacture of more resistant pieces and in this study, the pieces produced with non-dehumidified material obtained better results in the traction tests than the pieces produced with dehumidified material.

Comparing the tensile stress values obtained in the tests with the values taken from the datasheets of the materials (table 4 for PLA and table 7 for PETG), we can see that in the PLA, the stress values obtained, 47.47 MPa and 46.53 MPa, are higher than the tensile values of the datasheet, 32 MPa and for the PETG, the tensile values obtained, 49.46 MPa and 48.12 MPa, are very close to the tensile value of the datasheet, 47 MPa. As referenced earlier in the specimen construction layout in Figure 50, the PLA and PETG specimens had the same way of construction, horizontal or Y-X axis.

4.4. Cost/benefit of material dehumidification

With the growing concern of the industry regarding energy consumption, the reduction of production costs and carbon footprint is always an ultimate goal. With this, it becomes necessary to understand the energy cost of the processes involved in this work and its impact on the results obtained.

In this study, a different geometry was used from the previous geometries, because the previous geometries were fast for printing, which did not make it easy to collect data for the

cost analysis of the dehumidification and printing processes. The geometry used to determine the cost is shown in Figure 57.

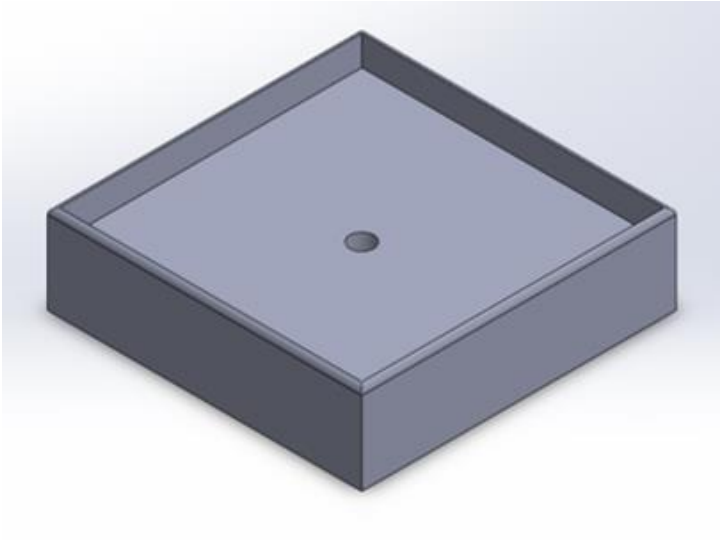

Figure 57 - Geometry used to determine the costs.

As in this case what was intended was a longer printing time, in which it was possible to obtain more realistic energy costs, the piece used was larger than the pieces used previously, as we can see in Figure 58.

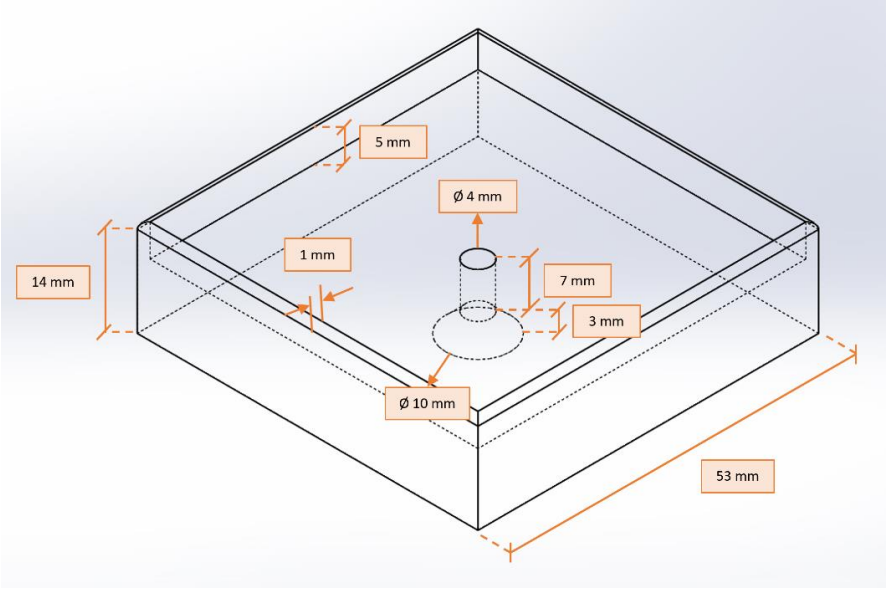

Figure 58 - Dimensions of the geometry used to determine the energetic costs.

In the energy cost analysis of the printed part, PLA material was used for data collection. The part was printed from a roll of filament with a total mass of 591 grams, whereas the mass of the spool supporting the material was 249 grams.

The piece in question had a printing time of approximately 1 hour, as the parameters are indicated in Table 20.

Table 20 - Parameters used to manufacture the part to determine energy costs.

Parameter Type	Metric	Value
Layers and perimeters	Layer height	0.2 mm
	First layer height	0.2 mm
	Shell thickness top	0.9 mm
	Shell thickness bottom	0.6 mm
Infill	Fill density	15%
	Fill pattern	Rectilinear
Speed	Perimeters	45 mm/s
	Infill	70 mm/s
	Top solid infill	45 mm/s
	Bridges	25 mm/s
Extruder	Nozzle diameter	0.6 mm
	Retraction length	0.8 mm
	Retraction lift Z	0.4 mm
Filament	Diameter	1.75 mm
	Nozzle temperature	215 °C
	Bed temperature	60 °C

The test consisted of collecting values in kWh of the energy consumption in the following processes:

- dehumidification;

- dehumidification with printing;

- printing.

The setup temperatures of the equipment used in the tests were 55 ºC for the dehumidifier, 215 °C for the printer nozzle, and 60 °C for the printer hot bed.

Table 21 depicts the collected data on the energy consumption of the processes.

Table 21 - Analysis of energy consumption.

Process	Elapsed time [h]	Total energy consumed [kWh]	kWh value [€]	Total cost [€]
Printing	1	0.10	0.15	0.01
Dehumidification	3	0.32		0.05
Dehumidification + printing	4	0.42		0.06

In Table 21 there is a relationship between the processes used, material drying and printing, and their energy consumption. It is possible to achieve the energy consumption of each process individually and the processes together. The elapsed time indicates the time when the value measurements occurred for the three cases, to create a temporal relationship and easy interpretation. The kilowatt-hour value indicates the average value of energy consumed in each case during one hour and the total energy consumed indicates the total value of energy consumed during each case. At the value of 0.15€/kWh, the total cost of energy used was determined.

Figure 59 shows the results from Table 21, allowing a quick appreciation of the trends of the variables.

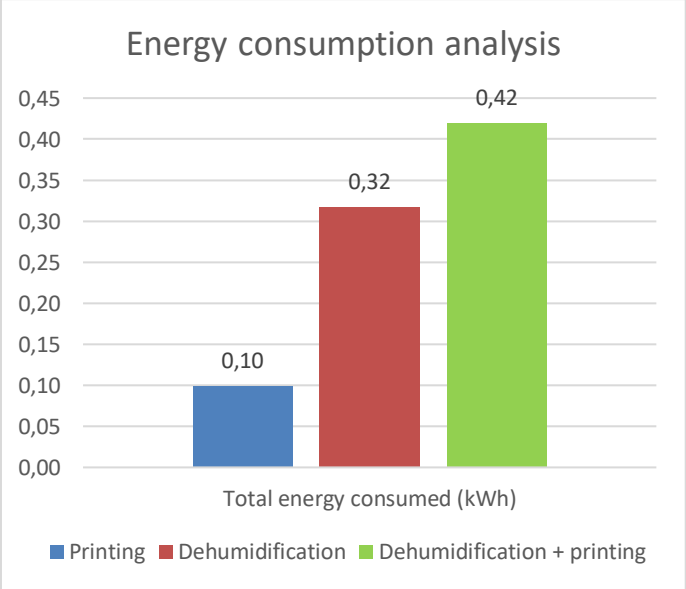

Figure 59 - Chart of the energy consumption analysis.

The kWh of electricity is based on the simple option for a contracted power of 6.9 kVA.

The dehumidifier took 18 minutes to reach the actual temperature of 50 ºC.

For the development of this experiment, a larger piece was used so that the data could be handled more easily. The piece has a mass of 68 grams in the simulation software and after printing, it weighed 64 grams. As previously mentioned, the raw material used was PLA, with a density of 1.22g/cm^3.

Energy costs are an important point in the decision between quality and production cost. The main objective of this test was to show the energy costs involved in these processes and the added cost of using a dehumidifier, which is seen as an added value for the improvement of the pieces obtained.

5. Results and discussion

The main goal of this work is to study the impact of the presence of moisture in the filament before its processing at an aesthetic level and in terms of mechanical performance, as well as the cost of this post-processing taking into account the benefit obtained at the end of the produced piece.

As for the aesthetic tests, the results obtained were as expected, where a stringing was observed in the pieces that were produced without dehumidification pre-processing of the material. In the case of prior dehumidification of the material for 3 hours and at the temperature recommended by the filament manufacturer, the stringing effect in the pieces were decreasing in the case of both PLA and PETG, a clear sign of the reduction of moisture in the filament. In the case of prior dehumidification of 6 hours of material, maintaining the recommended temperatures for each material, a reduction in the stringing effect was observed. In the results obtained it was possible to observe the effect of reducing the humidity in the filament, by the fact that there was a reduction in the stringing of material in the pieces produced in the 3 scenarios. The materials were tested using the dehumidification temperature recommended by the manufacturers, because the dehumidification time, of both materials, was one of the variables used for the tests, in order to understand the behavior of the material at the time of the manufacture of the pieces.

In the mechanical tests performed, the tensile strength of the specimens made of PLA and PETG showed similar behavior, because both specimens printed with non-dehumidified material show higher values than those printed with material dehumidified for 6 hours. In the case of PLA, the difference in mechanical strength between specimens printed under different conditions is approximately 2%, while in the case of PETG it is 3%. These results indicate that both materials have mechanical strength when printed with filament without pre-processing dehumidification. The specimens used in the tensile test were printed with a thickness of 6 mm instead of being printed with a thickness of 3.2 mm according to ASTM D638, but what was intended to be evaluated in the test would be the impact of moisture against the mechanical strength of the test specimens, because dimensionally the test specimens were equal.

The total energy consumed to dehumidify a roll of PLA with a total mass of 591 grams for 3 hours was 0.32 kWh, a low value when avoiding rework and visible defects in the printed parts. This value resulted from a test of the PLA raw material, which uses a low value of

dehumidification temperature, 50 °C. This value will increase for higher temperatures and dehumidification times.

The difference found in the mass of the pieces produced in which the material was dehumidified and the pieces in which the material was not dehumidified, in the case of PLA, the piece produced with material that was not dehumidified was 3.31 grams and the mass of the piece produced with material dehumidified for 6 hours showed a slightly higher mass, 3.44 grams. In the case of PETG, the scenario was the opposite, the piece printed with non-dehumidified material had a mass of 3.51 grams and the piece printed with the material previously dehumidified for 6 hours had a mass of 3.49 grams, slightly lower than the piece produced with non-dehumidified material. This difference in behavior between PLA and PETG may be due to the characteristics of each material, where the pieces printed in PLA increase their mass with the reduction of humidity in the filament used and PETG reduces the mass of the printed pieces with the reduction of humidity in the filament used. This subject could be studied in more detail in future works.

Regarding the diameter of the nozzle used in the printer, it may be an important factor to reduce the stringing effect during printing.

It was possible to obtain parts without stringing if the dehumidification time of the materials was respected, 8 hours at 50 °C for PLA and 8 hours at 60 °C for PETG, if the extruder nozzle diameter was reduced and if the shrinkage and material temperature parameters were changed.

For the preparation of the tests, the performance of the dehumidifier had an impact because, in order to obtain the average temperature inside the chamber of the equipment, it was necessary to program the installation temperature to 55 °C in the case of PLA, to be able to obtain a real average of about 50 °C inside, and 65 °C in the case of PETG to be able to obtain a real average of about 60 °C inside. The use of the Arduino was important in collecting the information on the real temperature inside the chamber to optimize the temperature according to the recommended one, being the difference between the setting temperature in the device and the real temperature inside the chamber of 5 °C.

6. Conclusion

This work proved the negative impact of the degradation of polymeric materials which, with processing, results in visual defects, but which at a mechanical level is not advantageous.

The results obtained through the Arduino came to prove the inefficiency of the filament dryer to reach the setup temperature. The positioning of the sensors inside the dryer showed the thermal differences inside the device between the top, middle and bottom, revealing thermal differences of 5 °C.

The results obtained demonstrate that the specimens produced, in PLA and PETG, have better behavior on tensile tests when they do not have pre-processing dehumidification. In this way, there is no decrease in properties regarding mechanical behavior, but there is a clear improvement in terms of processing and aesthetic appearance.

Regarding the aesthetic tests, we can conclude that the piece printed with PLA does not change its appearance significantly between the test with 3 hours of filament dehumidification compared to the piece printed with 6 hours of filament dehumidification. For PETG, the differences between the 3 hours of filament dehumidification and the 6 hours of filament dehumidification are evident, showing significant improvements.

In the weight of the pieces, we can conclude that the mass of PLA and the mass of PETG are inversely proportional to the dehumidification time of the material because PLA increases the mass of the pieces with the increase of the dehumidification time and PETG decreases the mass of the pieces with the increase of the dehumidification time. The simulation obtained by the CAD software and the slicer software are close to the values obtained in the pieces, where the CAD software presents a lower value and the slicer software a higher value.

In terms of energy costs, we can conclude that the use of the equipment has a low consumption when used with PLA. The main objective of this work was achieved, to facilitate the process and production of parts, using FDM, for users who are faced with these barriers.

Bibliography

[1] U. M. Dilberoglu, B. Gharehpapagh, U. Yaman, and M. Dolen, "The Role of Additive Manufacturing in the Era of Industry 4.0," *Procedia Manuf.*, vol. 11, no. June, pp. 545–554, 2017, doi: 10.1016/j.promfg.2017.07.148.

[2] L. T. Sin and B. S. Tueen, *Polylactic Acid A Practical Guide for the Processing, Manufacturing, and Applications of PLA*, vol. 53, no. 9. 2019.

[3] "ASTM D638: Test Method for Tensile Properties of Plastics - Safe Load Testing Technologies." https://www.safeloadtesting.com/astm-d638-test-method-for-tensile-properties-of-plastics/ (accessed Mar. 03, 2022).

[4] A. R. Torrado and D. A. Roberson, "Failure Analysis and Anisotropy Evaluation of 3D-Printed Tensile Test Specimens of Different Geometries and Print Raster Patterns," *J. Fail. Anal. Prev.*, vol. 16, no. 1, pp. 154–164, 2016, doi: 10.1007/s11668-016-0067-4.

[5] L. Da Xu, E. L. Xu, and L. Li, "Industry 4.0: State of the art and future trends," *Int. J. Prod. Res.*, vol. 56, no. 8, pp. 2941–2962, 2018, doi: 10.1080/00207543.2018.1444806.

[6] O. Diegel, A. Nordin, and D. Motte, *Additive Manufacturing Technologies*. 2019.

[7] L. Jyothish Kumar, P. M. Pandey, and D. I. Wimpenny, *3D printing and additive manufacturing technologies*. 2018.

[8] "The 7 categories of Additive Manufacturing | Additive Manufacturing Research Group | Loughborough University." https://www.lboro.ac.uk/research/amrg/about/the7categoriesofadditivemanufacturing/ (accessed Feb. 22, 2022).

[9] G. H. Loh, E. Pei, J. Gonzalez-Gutierrez, and M. Monzón, "An overview of material extrusion troubleshooting," *Appl. Sci.*, vol. 10, no. 14, 2020, doi: 10.3390/app10144776.

[10] H. Baş, S. Elevli, and F. Yapıcı, "Fault Tree Analysis for Fused Filament Fabrication Type Three-Dimensional Printers," *J. Fail. Anal. Prev.*, vol. 19, no. 5, pp. 1389–1400, 2019, doi: 10.1007/s11668-019-00735-6.

[11] C. Bell, “Maintaining and Troubleshooting Your 3D Printer,” *Maint. Troubl. Your 3D Print.*, 2014, doi: 10.1007/978-1-4302-6808-6.

[12] T. Box, “Make: Ultimate Guide to 3D Printing,” *Make:*, 2013, [Online]. Available: makezine.com.

[13] “Two Trees Sapphire Pro Review: Hands On | All3DP.” https://all3dp.com/1/two-trees-sapphire-pro-review-3d-printer-specs/ (accessed Mar. 03, 2022).

[14] “Creality Ender-3 Pro.” https://threed.store/creality-ender-3-pro (accessed Sep. 19, 2022).

[15] “NEVA Magis 3D Printer.” https://www.generationrobots.com/en/402771-neva-magis-3d-printer.html (accessed Mar. 03, 2022).

[16] P. Sovereignty, “Edition II,” 2019.

[17] “Filament Dryers Professional filament drying solution for open-materials 3D printers.”

[18] “Filament Dryer FD1 – Mass Portal.” https://massportal.com/home/filament-dryers/filament-dryer-fd1/ (accessed Jul. 25, 2022).

[19] “PrintDry Filament Dryer PRO - PrintDry™.” https://www.printdry.com/product/printdry-filament-dryer-pro/ (accessed Mar. 03, 2022).

[20] “Drywise In-Line Filament Dryer.” https://drywise.co/products/drywise-in-line-filament-dryer (accessed Jul. 25, 2022).

[21] “Thought3D, the producer of Magigoo introduces Drywise - A reliable, smart, inline filament dryer for FFF printers - Magigoo.” https://magigoo.com/blog/thought3d-the-producer-of-magigoo-introduces-drywise-a-reliable-smart-inline-filament-dryer-for-fff-printers/ (accessed Jul. 25, 2022).

[22] “Stringing or Oozing.” https://www.simplify3d.com/support/print-quality-troubleshooting/stringing-or-oozing/ (accessed Jul. 25, 2022).

[23] S. Kulkarni, *Robust process development and scientific molding: Theory and practice*. 2010.

[24] V. Mazzanti, L. Malagutti, and F. Mollica, “FDM 3D printing of polymers containing natural fillers: A review of their mechanical properties,” *Polymers (Basel).*, vol. 11, no. 7, 2019, doi: 10.3390/polym11071094.

[25] M. Applications, “Ingeo ™ Biopolymer 3D870 Technical Data Sheet 3D Printing Monofilament – High Heat and Impact Grade,” no. 4, pp. 1–4.

[26] M. A. Y. Be, F. Or, H. If, C. Skin, and E. Y. E. Irritation, “1 . Identification of the substance / preparation and of the company / undertaking 3 . Composition / information on ingredients,” pp. 1–7, 2007.

[27] T. Chen and J. Zhang, “Non-isothermal cold crystallization kinetics of poly(ethylene glycol-co-1,4-cyclohexanedimethanol terephthalate) (PETG) copolyesters with different compositions,” *Polym. Test.*, vol. 48, pp. 23–30, 2015, doi: 10.1016/j.polymertesting.2015.09.008.

[28] “Prusament PETG Jet Black 1kg | Original Prusa 3D printers directly from Josef Prusa.” https://www.prusa3d.com/product/prusament-petg-jet-black-1kg/#about-petg (accessed Mar. 03, 2022).

[29] “Original Prusa i3 MK3S+ 3D printer | Original Prusa 3D printers directly from Josef Prusa.” https://www.prusa3d.com/product/original-prusa-i3-mk3s-3d-printer-3/ (accessed Mar. 03, 2022).

[30] “ATmega2560 | Microchip Technology.” https://www.microchip.com/en-us/product/ATmega2560 (accessed Aug. 07, 2022).

[31] B. Susilo, M. B. Hermanto, R. Damayanti, and A. I. A. Putra, “The application of a data acquisition system and airflow control system in an air dehumidified drying machine,” *IOP Conf. Ser. Earth Environ. Sci.*, vol. 757, no. 1, 2021, doi: 10.1088/1755-1315/757/1/012025.

[32] “ELEGOO Mega 2560 The Most Complete Starter Kit Compatible with Arduino – ELEGOO Official.” https://www.elegoo.com/collections/mega-2560-starter-kits/products/elegoo-mega-2560-the-most-complete-starter-kit (accessed Mar. 03, 2022).

[33] M. Kusriyanto and A. A. Putra, “Weather Station Design Using IoT Platform Based On

Arduino Mega," *ISESD 2018 - Int. Symp. Electron. Smart Devices Smart Devices Big Data Anal. Mach. Learn.*, pp. 8–11, 2019, doi: 10.1109/ISESD.2018.8605456.

[34] "Buy Temperature and humidity sensor DHT22 Botland - Robotic Shop." https://botland.store/multifunctional-sensors/2637-temperature-and-humidity-sensor-dht22-am2302-module-cables.html (accessed Mar. 03, 2022).

[35] "Shelly Plug | Shelly Shop Europe." https://shop.shelly.cloud/shelly-plug-wifi-smart-home-automation#71 (accessed Mar. 03, 2022).

[36] "ZwickRoell Z100, pre-owned | ZwickRoell." https://www.zwickroell.com/products/pre-owned-market/pre-owned-z100-allroundline-100-kn/ (accessed Mar. 03, 2022).

[37] "Mettler Toledo AG 204 Analytical Balance | Marshall Scientific." https://www.marshallscientific.com/Mettler-Toledo-AG-204-Analytical-Balance-p/me-ag204.htm (accessed Sep. 24, 2022).

[38] "Standard Test Method for Tensile Properties of Plastics." https://www.astm.org/d0638-02.html (accessed Mar. 03, 2022).

[39] K. Durgashyam, M. Indra Reddy, A. Balakrishna, and K. Satyanarayana, "Experimental investigation on mechanical properties of PETG material processed by fused deposition modeling method," *Mater. Today Proc.*, vol. 18, pp. 2052–2059, 2019, doi: 10.1016/j.matpr.2019.06.082.